Response to the reviewers' comments

Response to the comments of Reviewer #1

General Comments:

Question 1: It is necessary and indispensable that the manuscript contains a detailed description of the formation and evolution of the planetary boundary layer.

Response: Based on your comments, we have concluded a detailed description of the formation and evolution of the planetary boundary layer in lines 41-61.

Question 2: The equation for the potential temperature difference (PTD) on line 115 is very vague and poorly understood. Authors should make a greater effort to characterize the physical criteria that allow choosing and safety to identify the types of the atmospheric boundary layer. It is important to consider that buoyancy effects make the convective and stable ABLs strikingly distinct.

Responses: Firstly, according to your suggestions, we have added statements to characterize the physical criteria that allow choosing and safety to identify the atmospheric boundary layer height. Secondly, we have added some explanations for the physical criteria of the PTD method to identify the types of the atmospheric boundary layer. The PTD method identifies the stable and convective boundary layers by judging the stability of the near surface layer atmosphere considering that buoyancy effects make the convective and stable ABLs strikingly distinct. Thirdly, we have added a detailed procedure for calculating the ABL height, the illustration of idealized atmospheric boundary layer (ABL) regimes and ABL height determination procedure, and some examples of the derived potential temperature (PT) profiles from soundings for the three types of ABL. The associated statements are in lines 137-172 and Fig. 2.

Question 3: the authors should consider in their analysis the fact that "The neutral ABL is rare because small virtual temperature differences in the ABL can cause large buoyancy patterns". How the authors identify this particular type of ABL? The authors also need to build vertical temperature and wind profiles and display them in the study.

Response: We have added the discussion for the physical criteria of the PTD method to identify the NBL and provided some examples of the derived potential temperature (PT) profiles from soundings for the three types of ABL (in lines 137-172 and Fig. 2).

Major comments

1. Line 115: The PTD classification is a fundamental criterium for the present manuscript. As a consequence, the authors must provide a more detailed discussion of the employed methodology to obtain the heights of the distinct ABL types. As the manuscripts basically observational data analysis, is not enough for the readers the citations presented.

Response: Following your suggestion, we have added a detailed description of the employed methodology to obtain the heights of the distinct ABL types and provided some examples of the derived potential temperature (PT) profiles from soundings for the three types of ABL. The associated statements are seen in lines 137-172 and Fig. 2.

2. Line 155: How a SBL can occur at noon (14:00 BJT). In this daytime period, there is a CBL. How the CBL height is near to the NBL height? The authors need to clarify.

Response: Our result shows that the SBL mainly occurs in the early morning, while the CBL mainly occurs at noon and in the late afternoon. The NBL does not show a remarkable diurnal variation. Nevertheless, the daytime SBL and the night-time CBL may also occur with low frequencies in the TP, which is likely due to the 'abnormal' forcing associated with certain synoptic conditions or cloud coverage (Medeiros et al., 2005; Poulos et al., 2002; Stull, 1988). See lines 230-235.

Stull (1998) and Blay-Carreras et al. (2014) revealed that the NBL often occurs in the transition periods between the CBL and the SBL. Since these transitions occur rapidly, the NBL may have the same characteristics in the state variables as the CBL prior to the transition although the dynamic forcing in the NBL maybe weaker compared to the CBL. Our result also shows that the CBL and NBL heights display the similar character. This result is consistent with those from Zhang et al (2017). See lines 254-258.

In addition, the similarity between the CBL and NBL may also be related to the ABL type identification scheme. The neutral stratification condition ($\sigma = 0$) is rare in nature. In our calculation, the threshold value of the NBL is set to -1.0 to 1.0, which is consistent with Liu and Liang (2010). Consequently, some SBLs and CBLs with weak stratification will be identified as NBLs. See lines 150-152.

Minor comments:

1. abstract "The SBL accounts for 85% of the TP ABL. At noon, there is a wide distribution in the ABL height up to 4000 m. The CBL accounts for 77% of the TP ABL, with more than 50% of the CBL height above 1900 m." Please rewrite more clearly this statement. For this reviewer the above statistics are confused.

Response: Thanks. Indeed, our statements should add the time frame to avoid any possible misunderstanding. According to your comments, we have changed (in lines 19-23).

2. Line 24: The authors need to present a better definition of the ABL.

Response: Based on your comments, we have modified the definition of the ABL (in lines 31-35).

3. Line 154: Please correct the hour "00:80 BJT"

Response: We have corrected (in line 224).

Response to the comments of Reviewer #2

Main concerns:

1. Although the presentation of the manuscript has good logic flow, descriptions of the data processing or the results can be confusing at places. The clarity of the manuscript can be improved. I have made some specific suggestions listed in the minor concerns, but the authors should go through the manuscript very carefully or get help from people experienced in writing scientific articles in English.

Response: According to your suggestions, we have modified the text listed in your minor concerns and carefully revised the language.

2. The manuscript can be enhanced if the methodology in defining the ABL types using the PTD are revisited in the discussion section. For the SBL, the mode of the ABL height is around 300 m, suggesting that the PTD represents the temperature gradient in the main body of the stable ABL. For the CBL, since few measurements shows CBL height less than 500 m (except at 20:00 BJT), the 50 m height is likely within the surface layer. The 250 m level, on the other hand, can be in the surface layer or in the well-mixed portion of the CBL depending on the CBL height (assuming the surface layer is ~10% of the ABL). The PTD in this case represent approximately the potential temperature difference in the surface layer or between the surface and the well-mixed CBL. The meaning of the PTD for the NBL should be similar to that in the CBL except with a smaller temperature difference. Clarifications like this should be helpful to the readers.

Also, how sensitive are the results to the choice of σ? My general feeling is that their results are not sensitive to the choice of σ since the results of the CBL and NBL are very similar. However, the authors should make appropriate comments on the sensitivity issue.

Response: Firstly, according to your suggestions, we have added statements to characterize the physical criteria that allow choosing and safety to identify the atmospheric boundary layer height.

Secondly, we have added some explanations for the physical criteria of the PTD method to identify the types of the atmospheric boundary layer. Thirdly, we have added a detailed procedure for calculating the ABL height, the illustration of idealized atmospheric boundary layer (ABL) regimes and ABL height determination procedure, and some examples of the derived potential temperature (PT) profiles from soundings for the three types of ABL. The associated statements are in lines 137-172 and Fig. 2.

Meanwhile, according to your suggestions, we have added the appropriate comments on the sensitivity issue of the σ in lines 150-152 and 165-166.

3. The overall results in this manuscript is consistent with the diurnal evolution of the ABL with the daytime deep CBLs and night-time shallow SBL. There are also occurrences of daytime SBLs and night-time CBLs although the frequencies of occurrence for both are small. The daytime SBL or night-time CBL are likely results of 'abnormal' forcing associated with certain synoptic conditions or cloud coverage. The authors mentioned a few times throughout the manuscript about the 'diurnal variations' of the SBL or the CBL (e.g., Lines 276, 290). These wordings are misleading and should be revised. It would be interesting to look into the mechanisms of the occurrence of daytime SBL and night-time CBL, but it may be beyond the scope of this paper.

Response: Thank for your comments. According to your suggestions, we have changed the "diurnal variations" to "temporal variations" and added this comment. The associated statements are seen in lines 230-235, 237, 241, and 377.

Minor points:

1. Line 14: 'The SBL accounts for 85% of the TP ABL' should add the time frame here to avoid misunderstanding: 'The SBL observed during this time accounts for 85% of the TP ABL'

Response: We have changed in line 19.

2. Line 15: 'The ABL height exhibits….', again, need to specify time: 'The ABL height at noon exhibits…'

Response: We have changed in line 20.

3. Line 20: 'For the western (eastern) TP…' , make it 'In general, for the western (eastern) TP…'

Response: We have modified the text (in line 26).

4. Line 28: change 'convective transmission' to 'convective transport'.

Response: We have changed (in line 36).

5. Line 56: change 'have addressed' to 'found'; also change 'can be as high as 2000–3000 m' to 'can reach 2000–3000 m'.

Response: We have modified the text (in line 78).

6. Line 57: change 'Song et al. (1984) examined the ABL height at Gaize station of the western TP is above 3000 m, while the ABL heights….' To 'Song et al. (1984) found the ABL height at Gaize station of the western TP to be above 3000 m, while the ABL heights….'

Response: It has been changed in lines 80-81.

7. Line 62: 'These results show that the ABL height over the TP varies greatly with position and season'. Change 'position' to 'location'.

Response: We have changed in line 80.

8. Line 67: change 'and less-developed logistics' to 'logistic challenges'.

Response: It has been changed in line 89.

9. Line 68: remove 'a short-time experimental' from the sentence. Also change 'Thus the interpretation of their results has certain limitations' to 'Thus, the statistical representation of their results is limited'.

Response: It has been changed in line 91.

10. Line 70: change 'climatic conditions' to 'general climate'.

Response: It has been changed in line 92.

11. Line 72: change 'beginning in 2013 has deployed routine sounding systems at Shiquanhe, Gaize, and Shenzha stations of the western TP (Fig. 1)' to 'has made routine sounding launches at Shiquanhe, Gaize, and Shenzha stations of the western TP (Fig. 1) since 2013'.

Response: It has been changed in lines 94-95.

12. Line 82: change 'Section 4 gives major factors…' to 'Section 4 examines major factors…'

Response: It has been changed in line 106.

13. Line 94: change 'After the quality of the sounding observational data, we finally select the periods from 15 June to 31 July 2013, from 15 June to 31 August 2014, and from 1 June to 31 August 2015 in this study' to 'After quality control of the sounding data, we selected data from three time periods for this study: 15 June to 31 July 2013, 15 June to 31 August 2014, and 1 June to 31 August 2015'.

Response: It has been changed in lines 118-120.

14. Line 95: change 'There are a total of 11,635 sounding profiles (Fig. 1a) and 4757, 2049, and 4841 profiles separately at 08:00 BJT (Fig. 1b), 14:00 BJT (Fig. 1c), and 20:00 BJT (Fig. 1d) for 19 stations over the TP' to 'There are a total of 11,635 sounding profiles (Fig. 1a) from 19 stations

over the TP region consisting of 4757, 2049, and 4841 profiles at 08:00 BJT (Fig. 1b), 14:00 BJT (Fig. 1c), and 20:00 BJT (Fig. 1d), respectively'. Note the numbers do not add up to the total here.

Response: We have modified the text in lines 120-122.

15. Lines 97 and 101: change 'sample number' to 'sample size'.

Response: It has been changed in lines 122, 123, and 127.

16. Line 99: 'Thus we also select the operational observation records that correspond to the intensive observation records'. Unclear sentence. Did you mean you subsampled the original dataset to only take those soundings that were made at the time when soundings of the test group dataset were made?

Response: According to this comments, we have modified the text. See lines 125-127.

17. Line 105: change 'few obstacles' to 'few vegetation'.

Response: It has been changed in line 130.

18. Line 107: change '02:00 BJT, 08:00 BJT, 14:00 BJT, and 20:00 BJT' to '02:00, 08:00, 14:00, and 20:00 BJT'.

Response: It has been changed in lines 132-133.

19. Line 110: Needs to give more details on how the interpolation of the original sounding data were made? Any filtering or smoothing during the interpolation process?

Response: We have modified the text. See lines 144-146.

20. Line 117: 'For both the CBL and NBL, the ABL height is calculated as the height at which an air parcel rising adiabatically from the surface becomes neutrally buoyant (Stull 1988)'. To be

clear about what you are doing, you may want to add: 'Practically, the ABL height is the level where it potential temperature is the same as that at the lowest sounding level'. You also need to clarify the definition of the SBL height. I believe you use the height of maximum wind in the LLJ, not the 'maximum wind shear'.

Response: According to your suggestion, we have added a more detailed discussion about the employed methodology to obtain the CBL height and revised the definition of the SBL height. See lines 154-169.

21. Line 123: change 'and diurnal transitions (from day to night and from night to day)' to 'and day/night transitions'.

Response: It has been changed in line 175.

22. Line 125: how do you define the 'local standard time' for this location?

Response: We use the local solar time as the LST and add this statement in line 177.

23. Line 144: 'the ABL height continues to increase in the WTP'. Is the mean height greater than 14:00 BJT to justify the 'continues to increase'? It does not look like it in the figure.

Response: We have changed in lines 200-202.

24. Line 150: 'The ABL height reaches the maximum in the late afternoon.' This is not clearly seen in the data in Figure 2. You may want to change to: 'Figure 2 shows continued increase in BLH in the west-most stations from 14:00 to 20:00 BJT.'

Response: According to your suggestion, we have modified. See lines 205-206.

25. Line 165: 'Figure 4 shows the distribution of occurrence frequency of different ABL types at 08:00 BJT, 14:00 BJT, and 20:00 BJT. It is clear that the occurrence frequency shows significant

diurnal variations for the SBL and CBL'. This statement is misleading. There should not be diurnal variation of SBL and CBL. The results are simply consistent with the diurnal evolution of the ABL with prevalent CBL during the sunlight hours and SBL at night. Similarly, the discussion of the 'diurnal variation' of NBL should be done with caution. It also would be helpful to provide the sunrise and sunset hours at representative sites of WTP and ETP to illustrate the time difference in the CBL SBL or SBL CBL transition. See also my comments in the list of 'Major Concerns'.

Response: According to your suggestions, we have changed in lines 225, 229, 237, and 241. Moreover, we have added this comments in the discussions in lines 230-235.

26. Line 209: why are the RMSE in percentage here?

Response: This RMSE is for the occurrence frequency. In our revised manuscript, we have changed "with root-mean-square errors (RMSEs) between 1.1% and 2.7%" to "with root-mean-square errors (RMSEs) of the occurrence frequency between 1.1% and 2.7%" in lines 282-283.

27. Line 216: change 'larger NBL and CBL heights' to 'deeper NBLs and CBLs'.

Response: It has been changed in line 291.

28. Line 221: change 'A lot of studies' to 'Many previous studies'.

Response: It has been changed in line 295.

29. Line 225: change '…observations at SQH, NQ, and LZ stations, analyzing the…' to '…observations at SQH, NQ, and LZ stations to analyze the…'

Response: It has been changed in line 300.

30. Line 228: Any reasons for doing the '6-hour mean' in Figure 8? Which 6-hour window did you use, or was it a running mean? Please clarify.

Response: We have added the reasons for doing the '6-hour mean' and modified the text in lines 308-310.

31. Line 230: remove 'That is'. Change 'which supports the…' to 'which is consistent with the…'.

Response: It has been changed in line 312.

32. Line 233: 'The maximum value of SHF is…'. You should use the mean values, not the maximums.

Response: It has been changed in lines 315-316.

33. Line 237: 'It is clear that the peak of the SHF diurnal variation occurs earlier compared to that of the ABL height at SQH station.' Unclear sentence. Reword.

Response: It has been changed. See lines 320-321.

34. Line 238: again, how was the LST defined?

Response: We use the local sidereal time as the LST and add this statement in line 177.

35. Line 239: 'This difference in SHF between SQH and LZ stations is possibly associated with more cloud cover (reducing the solar radiance at the surface)'. It is better to make your statement about cloud cover after the next paragraph, if it is true.

Response: We have deleted this content on cloud cover in lines 318-325 because it is discussed in the next paragraph.

36. Line 260-265: Good discussions about the soil moisture effects on SHF. What about latent heat flux (LHF)? Unless LHF is in general small, which may be true in your case for both WTP and ETP, it is also an important forcing for the ABL. But you should at least mention latent heat in this discussion.

Response: We have calculated the mean LHF at three stations (not included in the text). The result indicates that the kinematic moisture flux (KMF) is general small for both WTP and ETP. See lines 303-308.

37. Line 300: change 'That is, in' to 'In'.

Response: It has been changed in line 386.

38. Line 311: 'for providing the data available', delete.

Response: It has been changed in line 406.

39. Figure 1. Larger font size is needed for axis labels, station names, as well as the number of soundings. In figure caption: change 'Some letters are for the abbreviated names of stations. The green line is for the topography above 3 km.' to 'Some station names are given as abbreviations in (a) and the green lines shows the contour of terrain height at 3 km'.

Response: It has been changed in lines 571-573.

40. Figures 2 d,e, and f, needs larger font size for axis labels and legends.

Response: It has been changed in lines 583-587.

41. Figure 8 caption, change 'radiation flux' to 'irradiance'.

Response: It has been changed in line 614.

Response to the comments of Reviewer #3

1. Of course, authors did not bring up any discussion why the other seasons were missing in the manuscript.

Response: The TIPEX-III experiment carried out the intensive observations in the TP region at noon (14:00 BJT) during summer, which provide a better dataset for studying the ABL during summer. In other seasons, there are no observations at 14:00 BJT. Thus summer is selected in this study. The associated statements have been added in lines 93-100 and 116-118. In addition, a statement has been added in Summary and Discussion (in lines 402-404).

2. However, at many instances, the manuscript lacks the interpretation of the results.

Response: The original manuscript was structured to show the results in Section 3 and present physical explanations in Section 4. We have realized, based on your comments, that arrangement may result in disconnections between the results and their discussions. In the revised manuscript, we have included some interpretations and the possible physical reason analyses immediately following the results. See our response to question 16 for the specific revisions.

3. In the abstract: A big picture of the problem for the region for ABL research needs to be mentioned.

Response: According to your suggestion, we have added some statements about the existing problem for the TP ABL research in lines 9-11.

4. It is mentioned "The SBL accounts for 85% of the TP ABL" and also mentioned in the very next line, "The CBL accounts for 77% of the TP ABL" needs some clarification or needs to be rephrased. Otherwise, they contradict in general sense.

Response: Thanks. Indeed, our statements should add the time frame to avoid any possible misunderstanding. According to your comments, we have changed (in lines 19-23).

5. The ABL height exhibits a large west-east difference, with a mean height above 2000 m in the western TP and around 1500 m in the eastern TP." Did you refer to the daytime well-mixed CBL here?

Response: It is due to our unclear statement. This sentence is for ABL not only for CBL (in line 21).

6. In the numbers, authors need to mention whether this is m AGL or m MSL. Since spatial variability is mentioned underlying orography will play a role if these numbers are in MSL. Please clarify.

Response: It is m above ground level (AGL). Following your suggestion, we have changed "m" to "m AGL" in the revised manuscript.

7. Line 30: "ABL height in climate prediction". Authors need to bring an appropriate reference here. There is only one study that directly refers to climate projection. Please refer to the following one: "Differences in the efficacy of climate forcings explained by variations in atmospheric boundary layer depth"

Response: We have added the associated references on the ABL height in climate prediction (in lines 37-38).

References:

Garratt, J. R., 1993: Sensitivity of climate simulations to land-surface and atmospheric boundary-layer treatments—A review. J. Climate, 6, 419–448.

Esau, I., and S. Zilitinkevich, 2010: On the role of the planetary boundary layer depth in the climate system. Adv. Sci. Res., 4, 63–69.

Davy, R., and I. Esau, 2016: Differences in the efficacy of climate forcings explained by variations in atmospheric boundary layer depth. Nat. Commun., 7, 11690.

8. Line 41: "The ABL height can be calculated from temperature, humidity, and wind profiles (Seibert et al., 2000; Seidel etal., 2010; Davy, 2018)." Please add a reference for numerical simulation as well since researchers are using models as well for this purpose.

Response: We have added the following references for numerical simulation (in lines 63-64).

References:

Holtslag, B. and B. A. Boville, 1993: Local versus nonlocal boundary-layer diffusion in a global climate model. J. Climate, 6, 1825–1842.

Bosveld, F. C., and Coauthors, 2014b: The third GABLS intercomparison case for evaluation studies of boundary-layer models. Part B: Results and process understanding. Bound-Layer Meteor.,152, 157–187.

9. Line 48: "solar altitude angle with respect to latitude" Please refer to Seidel et al., 2010.

Response: We have changed (in lines 68-70).

10. Line 69: "result has certain limitations" What are those? Please be specific here.

Response: According to another reviewer's suggestion, we have changed "Thus, the statistical representation of their results is limited" (in line 91).

11. Line 94: Quality check

Response: It is due to our mistake. We have changed to "quality control" (in line 119).

12. Line 108: "operational observation of total cloudiness" Are these from reanalysis or from ceilometers?

Response: It is the manual ground-based cloud cover observations from the China Meteorological Administration, and has been used to analyze the relationship between the ABL height and cloud cover in China by Guo et al. (2016) and Zhang et al. (2017). The associated statements are seen in lines 132-134.

References:

Guo, J. P., Miao, Y. C., Zhang, Y., Liu, H., Li, Z. Q., Zhang, W. C., He, J., Lou, M. Y., Yan, Y., Bian, L. G., Zhai, P. M.: The climatology of planetary boundary layer height in China derived from radiosonde and reanalysis data, Atmospheric. Chemistry. and Physics., 16, 13309-13319, doi:10.5194/acp-16-13309-2016, 2016.

Zhang, W., Guo, J., Miao, Y., Liu, H., Yang, S., Fang, Z., He, J., Lou, M. Y., Yan, Y., Li, Y., Zhai, P. M.: On the summertime planetary boundary layer with different thermodynamic stability in China: a radiosonde perspective, Journal of Climate., 31, doi: 10.1175/jcli-d-17-0231.1, 2017.

13. Line 150: "This west-east difference increases from noon to the late afternoon." Authors need to bring the concept of west-to-east march of the solar timing given span of 20 deg longitude would cause some "real" solar timing issue although in the region there is no time zone separations and BJT is used here. According to classical rule of "15 degrees of longitude per hour", it will result in at least local time difference of 80 minutes or little more from western site to eastern site. Thus, the increase in the west-east gradient is also attributed to some extent to this "real" local timing differences. See Seidel et al. 2010 and other relevant studies as well. Additionally, authors need to acknowledge the above-mentioned topic in other discussion where they brought up the west-east gradient changes from noon to late afternoon.

Response: We agree with you that the increase in the west-east gradient of ABLH (including CBL height and NBL height) from noon to the late afternoon is also attributed to some extent to the "real" local timing differences. According to Seidel et al. (2010, 2012) and Guo et al. (2016), in the revised manuscript, we have added an explanation for the increasing west-east difference of the ABLH over the TP from noon to the late afternoon (in lines 205-210).

In addition, the phenomenon of "the SBL/CBL mainly occurring in the ETP/WTP at 20:00 BJT" is also related to the above-mentioned topic. In the revised manuscript, we have added an explanation, that is, the above results are consistent with the diurnal development of the ABL structure including the SBL in the early morning, the CBL at noon, and different types of ABLs between the eastern and western TP in the late afternoon because of the latitudinal difference and the resultant difference in local solar times.

Note that the observations were made simultaneously for all stations. The associated statements are seen in lines 230-233.

14. Figure 3a-c shows the spatial distribution of the SBL height" How did they classify SBL regime during daytime soundings? Please clarify.

Response: The definition of the daytime SBL height is the same as that of the nighttime SBL in Section 2.2. In this revision, we have given the identification method of SBL in detail, the corresponding diagram of SBL, and an example (in lines 137-150, 167-172, and Fig. 2).

15. "remarkable diurnal variation." This is a qualitative statement unless some other SBL regimes are referred here for the contrasting scenario since SBL variability is in general low. Did you refer to the spatial variability? Please justify the causes for this then!

Response: We agree with you that the SBL variability is in general low, which is consistent with our results. We have changed in lines 261-263.

16. Throughout the results section, authors need to bring some discussion of the causes for these findings. Otherwise, it appears as reporting of the observed variability.

Response: Following your suggestion, we have brought some discussions of the causes in the third section. A detailed physical discussion has been given in the fourth section. The detailed statements are as follows. We have added an explanation for the regional difference of the ABLH over the TP at 14:00 BJT (in lines 196-198), an explanation for the increasing west-east difference of the ABLH over the TP from noon to the late afternoon (in lines 206-210), an explanation for the results of spatial and temporal distribution of occurrence frequency of different types of ABL (in lines 230-235), and a discussion for the results of temporal variations of all types of ABLH over the TP (in lines 254-258).

17. For section "3.2 Characteristics of SBL, NBL, and CBL heights" I will highly recommend authors performing the analyses of ABL depth growth rates which is most appropriate parameters that they wanted to discuss mentioned in the title and the abstract. Please see the feasibility of applying estimation of daily ABL depth growth rates.

Response: According to your suggestion, we have added the growth rates of the ABLH from 08:00BJT to 14:00 BJT and from 14:00 BJT to 20:00 BJT, and added the associated statements (in lines 212-220) and Fig. 4.

18. Several discussion via the frequency distribution analyses for ETP/WTP, authors need to decide the aim of these analyses. The results are presented with respect to findings and results without taking care of their interpretations.

Response: The analyses of the frequency distribution of ABLH (Fig. 6g, h) intend to show the differences between the two regions of the TP from a different angle than the differences in the mean ABLH shown in Fig. 7. This discussion focused on the most frequently observed ABLH and how these most common ABLH varied gradually from EPT to WPT. It is true that we have not included much physical interpretation here. However, discussions are added later when the boundary layer forcing factors are discussed in section 4. The text has been modified to make our objectives of the discussion clear (in lines 271-277).

19. Interpretation part. Line 23: "when SHF is strong, the turbulent motion is strong and the ABL height develops" True in general. What about the lag of ABL development since a number of studies showed that even after SHF attains its maximum daytime value, ABL depth growth continues till the time of early evening transitions. I would like to see some results in this respect between ETP and WTP and that will clearly illustrate the differences in the surface forcings the authors have tried to engage the readers.

Response: Thanks for your comments. Following your opinions, we have added the analysis of diurnal variations of SHF and ABLH. The associated statements are seen in lines 318-325.

20. Finally, authors should consider that some comparisons with regional scale variability of ABL depths (m MSL or m AGL, be consistent) should be presented and main conclusions why this study makes an unique contribution to the field emphasizing the new processes learned for very deep ABL over the region as reported in a number of past studies.

Response: As we understand for this question, we have compared the regional variability of the ABLH in TP with the other regional variability of the ABLH such as in the United States (Seidel et al., 2012) and in China (Guo et al., 2016) in the discussion (in lines 370-375 and 395-400), and also have explicitly stated the unique contribution of this study to the ABL in the TP (in lines 393-395).

Characteristics of the summer atmospheric boundary layer height over the Tibetan Plateau and influential factors

Junhui Che[1, 2, 3], Ping Zhao[1]

[1]State Key Laboratory of Severe Weather, Chinese Academy of Meteorological Sciences, Beijing, 100081, China
[2]College of Atmospheric Science, Nanjing University of Information Science and Technology, Nanjing, 210044, China
[3]Shandong Meteorological Service Center, Jinan, 250031, China

Correspondence to: Ping Zhao (zhaop@cma.gov.cn)

Abstract. The important roles of the Tibetan Plateau (TP) atmospheric boundary layer (ABL) in climate, weather and air quality have long been recognized, but little is known about the TP ABL climatological features and their west-east discrepancies due to the scarce data in the western TP. Based on intensive sounding, surface sensible heat flux, solar radiation, and soil moisture observational datasets from the Third Tibetan Plateau Atmospheric Scientific Experiment and the routine meteorological operational sounding and ground-based cloud cover ~~total cloudiness~~ datasets in the Tibetan Plateau (TP) for the period 2013-2015, we firstly investigate the west-east differences in summer ABL features over the TP and the associated ~~the features of summer atmospheric boundary layer (ABL) over the TP and its major~~ influential factors. It is found that the heights of both the convective boundary layer (CBL) and the neutral boundary layer (NBL) ~~show~~ exhibit ~~remarkable~~ a diurnal variation~~s~~ and a west-east difference ~~over~~ in the TP, while these features are not remarkable for the stable boundary layer (SBL) ~~diurnal variation is weak~~. Moreover, the ABL shows significant discrepancies in the amplitude of the diurnal variation and the persistent time of the development between the eastern and western TP. In the early morning, the ABL height distribution is narrow, with a mean height below 450 m above ground level (AGL) and a small west-east difference. The SBL observed at this moment accounts for 85% of the TP total ABL. At noon, there ~~is~~ are a wide distribution in the ABL height up to 4000 m AGL and a large west-east difference of the ABL height, with a mean height above 2000 m AGL in the western TP and around 1500 m AGL in the eastern TP. The CBL accounts for 77% of the TP total ABL at this moment, with more than 50% of the CBL height above 1900 m. ~~The ABL height exhibits a large west-east difference, with a mean height above 2000 m in the western TP and around 1500 m in the eastern TP.~~ In the late afternoon, the CBL and SBL dominate the western and eastern TP, respectively, which ~~resulting~~ results in a larger west-east difference of 1054.2 m between the western and eastern TP. The high ABL height in a cold environment over the western TP (relative to the plain areas) is similar to that in some extreme hot and arid areas such as Dunhuang and Taklimakan Deserts. In general, ~~For~~ for the western (eastern) TP, there is low (high) total cloud coverage, with large (small) solar radiation at the surface and dry (wet) soil. These features ~~result in~~lead to high (low) sensible heat flux and thus promotes (inhibits) the local ABL development. This study provides new insights for west-east structures of the summer ABL height, occurrence frequency, and diurnal amplitude over the TP region and the associated reasons.

1 Introduction

The Atmospheric boundary layer (ABL) commonly refers to the bottom layer of the troposphere ~~that is~~ directly coupled with the earth's surface at ~~affected by the underlying surface conditions with~~ a response time scale of about one hour or less , in which a variety of complex motions characterized by turbulence may be present (Stull, 1998). The turbulent motions in the ABL are responsible for the atmospheric mixing processes, which affects the vertical redistribution of water vapour, momentum, heat, and atmospheric pollutants ~~The ABL, as the interface for the exchanges of water vapour, momentum, heat, and matter between the surface and the free atmosphere, plays important roles in weather, climate, and the transport of air pollution~~ (Stull, 1988; Garratt, 1992; Huang et al., 2007; Miao et al., 2015). The ABL height (ABLH) as a fundamental variable is critical to ~~a key variable for diagnosing~~ diagnose turbulent mixing, vertical disturbance, convective transport~~transmission~~, ~~atmospheric~~ pollutant dispersion, and atmospheric environmental and effective heat capacity (Garratt, 1993; Seibert et al., 2000; Guo et al., 2009; Esau and Zilitinkevich, 2010; Dai et al., 2014; Pal et al., 2015; Davy and Esau, 2016). Therefore, the accurate specification of the ABL height is essential to develop weather, climate, and air pollution prediction models.

The cloud-free ABL overland can ~~generally~~ be divided into three types, that is, the convective boundary layer (CBL), the stable boundary layer (SBL), and the neutral boundary layer (NBL) (Stull, 1998). The CBL usually has the strongest turbulence forced by surface buoyancy flux with or without wind shear, and is generally capped by a strong temperature inversion maintained through large-scale subsidence. The CBL height is a result of the balance of the turbulence-induced entrainment and the subsidence velocity (e.g. Driedonks and Tennekes, 1984). However, turbulence in the SBL is mainly driven by the mean wind shear against negative buoyancy flux from the stable thermal stratification within the nocturnal surface inversion (NSI). The SBL height is hence related to the boundary layer wind and wind shear, which sometimes are used to identify the SBL height. The NBL occurs in neutral conditions with the turbulence of almost the same intensity in all directions (Stull, 1988; Blay-Carreras et al., 2014). It denotes the type of boundary layer with solely wind forcing and normally occurs during the transition from the daytime CBL to the night time SBL. It can also occur anytime when the buoyancy forcing is weak. The ABLH variability is dominated by its strong diurnal cycle (Stull, 1988; Garratt, 1992). In this diurnal cycle, the different manifestations of an ABLH are generated in response to the distinct forcing mechanisms that originate from mechanical (wind shear) and thermal (buoyancy) effects (Stull, 1988; Garratt, 1992). Over land and after sunrise, the surface is heated by solar radiation, resulting in upward heat flux that initiates strong updrafts of warm air. Such a mechanism generates a deepening of the CBL (Chen et al., 1997). At sunset, the surface cools more rapidly compared to the air above, resulting in negative heat flux that consumes turbulent kinetic energy. Consequently, shear-driven turbulence can only maintain a shallow SBL with the formation of the NSI (Zhang et al., 2011a; Miao et al., 2015). Above the NSI, the convective energy-containing eddies start to lose their strength and mixing capacity. This deep and near-adiabatic vertical region, which is the remnant of the daytime CBL, is known as the residual layer (RL). The use of precise information on the

RL in numerical models is of fundamental importance when describing the evolution of the diurnal CBL (Blay-Carreras et al., 2014; Chen et al., 2016).~~During the daytime, when sufficient solar radiation reaches the surface, the CBL usually dominates (Chen et al., 1997), with unstable thermal stratification and vigorous turbulence. At night, infrared cooling at the surface results in the nocturnal SBL (Zhang et al., 2011a; Miao et al., 2015), with ground-based temperature inversion and weak turbulent motion. The NBL occurs mainly in high wind conditions, particularly combining with thick and extended cloud coverage, and also occurs during the sunrise and sunset transition periods, with turbulence of almost the same intensity in all directions (Blay-Carreras et al., 2014).~~

The ABLH ~~height~~ can be calculated from temperature, humidity, and wind profiles (Holtslag and Boville, 1993;Seibert et al., 2000; Seidel et al., 2010; Bosveld et al., 2014; Davy, 2018). The CBL height is generally less than 2000–3000 m AGL and the SBL thickness is not more than 400–500 m AGL (Garratt, 1992). The ABL height shows an obvious spatial variation due to differences in topography, thermal properties of the underlying surface, and weather conditions. For example, the CBL can grow to ~~as high as~~the height of 4700 ~~m~~m AGL in New Delhi before the outbreak of the South Asian monsoon, whereas it ~~may~~ only reaches 900 ~~m~~m AGL in Bangalore during the monsoon period (Raman et al., 1990). Seidel et al. (2010, 2012) pointed out that a large east-west spatial gradient of the ABLH ~~height~~ at sunset in the United States spanning several time zones may be conflated with the diurnal variations of the ABL for the local solar time in the west earlier than in the east at fixed observation times~~may be related to a difference in the solar altitude angle with respect to latitude~~. Guo et al. (2016) identified three large-scale spatial ABLH patterns ~~in the ABL height~~ in China, that is, a west-east gradient during sunrise, an east-west gradient during sunset, and a south-north gradient at noon. The reasons for the first two patterns are similar to those observed in the United States shown in Seidel et al. (2012), while the south-north gradient may be related to local surface and hydrological processes (Guo et al., 2016; Zhang et al., 2017).

The Tibetan Plateau (TP) with an average elevation exceeding ~~4500~~ 4000 m is characterized by ~~has~~ complex land surface processes and boundary layer structures (Tao and Ding, 1981; Yanai and Li, 1994; Xu et al., 2002; Yang et al., 2004; Li et al., 2007; Sun et al., 2007; Zhao et al., 2018). The ~~ABL height~~ABLH in the TP can reach 2000–3000 m AGL, ~~is~~ generally higher compared to some plains areas (with the ~~ABL height~~ABLH of 1000–1500 m AGL) (~~Zhao et al., 1992). Some studies have addressed that the ABL height in the TP can be as high as 2000–3000 m (~~Ye et al., 1979; Zhao et al., 1992; Xu et al., 2002; Zhang et al., 2003). The ABLH in the TP varies greatly with location and season. At Gaize station of the western TP, the super-thick ABLH may exceed 5000 m AGL during winter (Chen et al., 2013, 2016). In the central TP, the ABLH is lower, between 400 and 1800 m AGL at Dangxiong station and 1750 m AGL at Namucuo Lake (Li et al., 2000; Liu et al., 2001, and Lü et al., 2008). ~~Song et al. (1984) examined the ABL height at Gaize station of the western TP is above 3000 m, while the ABL heights obtained by Li et al. (2000), Liu et al. (2001), and Lü et al. (2008) are lower in the central TP (between 400 m and 1800 m at Dangxiong station and 1750 m at Namucuo Lake).~~ Moreover, there is also a significant difference in the TP ~~ABL height~~ABLH ~~over the TP~~ between dry and rainy seasons (Zuo et al., 2004). For instance, ~~Li et al.~~

~~(2011) found that~~ the ~~ABL height~~ABLH at Naqu station is 2211–4430 m AGL in the dry season, ~~and~~ while it is 1006–2212 m AGL in the rainy season (Li et al., 2011)~~. Chen et al. (2013, 2016) observed the super thick ABL at Gaize station during winter, with the ABL height above 5000 m.~~. ~~These results show that the ABL height over the TP varies greatly with position and season.~~

Although observations ~~in the TP~~ and studies for ~~on~~ the ~~local~~ TP ABL features have made progress, routine meteorological operational sounding observations are scarce ~~over~~ in the western TP ~~, owing~~due to ~~its~~ the local high elevations, naturally harsh environmental conditions, and ~~less developed~~ logistics challenges. The previous studies on the ABL ~~over~~ in the western TP are usually based on observational data at Shiquanhe (during 15 days in one summer) and Gaize (during 22 days in one summer) stations ~~often based on a short-time experimental observational data at Gaize in one summer~~ (Song et al., 1984; Chen et al., 2013). Thus, the statistical representation of their results is limited~~ the interpretation of their results has certain limitations~~. Moreover, there are significant differences in surface properties and general climate ~~climatic conditions~~ between the eastern and western TP (Wang et al., 2016). ~~However, f~~Few studies ~~have~~ examined ~~this~~ the west-east difference in the ABLH features due to the scarce data in the western TP. To obtain a longer observational data in the western TP, the Third Tibetan Plateau Atmospheric Scientific Experiment (TIPEX-III) ~~beginning in 2013~~ has ~~deployed~~ made routine sounding ~~systems~~ lauches at Shiquanhe, Gaize, and Shenzha stations of the western TP (Fig. 1) since 2013, which fills in the data gaps in the operational sounding network over the western TP (Zhao et al., 2018). Meanwhile, the TIPEX-III also carried out the intensive sounding observations in the TP and adjacent stations at 14:00 Beijing Time (06:00 UTC) in June, July, and August (Zhao et al., 2019b). Compared ~~to~~ the previous field experiments over the TP, the TIPEX-III has a wider and longer coverage of sounding observations over the western TP, providing valuable observational data for studying the ABL features in the western TP and the west-east differences of these features in the TP during summer.

This study utilizes the TIPEX-III sounding observational data to investigate the features of the ~~ABL height~~ABLH ~~over~~ in the TP ~~, compares~~ and their differences ~~in the ABL height~~ between the western and eastern ~~parts of the~~ TP during summer, and analyzes the major factors affecting the ~~ABL height~~ABLH in the TP. The remainder of this paper is organized as follows. Main features of data and methods are described in Section 2. In Section 3, the characteristics of the ~~ABL height~~ABLH ~~over~~ in the eastern and western TP and their regional differences are analyzed in detail. In ~~Section~~ section 4, ~~gives~~ the major factors affecting the ~~ABL height~~ABLH ~~over~~ in the TP and the west-east differences are examined. Discussions and conclusions are given in Section 5.

2 Data and analysis methods

2.1 Observation data

The TIPEX-III carried out the intensive routine meteorological sounding observations at Shiquanhe (SQH), Gaize (GZ), and Shenza (SZ) stations of the western TP (marked by red dots in Fig. 1) since the 2013 summer (Zhao et al., 2018), ~~. These intensive observations~~which have been applied in research on the vertical structure of the upper troposphere and lower stratosphere at Gaize station during the rainy season and effects of assimilating the intensive sounding data on downstream rainfall (Hong et al., 2016; Yu et al., 2018; Zhao et al., 2018; Zhao et al., 2019b). These intensive sounding data and the routine meteorological operational sounding data at 16 stations of the central-eastern TP from the China Meteorological Administration (marked by black dots in Fig. 1) are utilized in this study. The sounding observations at the above intensive and operational sounding stations were carried out at 08:00 Beijing Time (BJT; 00:00 UTC), 14:00 BJT (06:00 UTC), and 20:00 BJT (12:00 UTC) each day during summer (June, July, and August)~~for the above intensive and operational sounding stations~~, including vertical profiles of temperature, humidity, and wind direction and speed. After the quality control of the sounding observational data, we ~~finally~~ select data from three time~~the~~ periods for this study: ~~from~~ 15 June to 31 July 2013, ~~from~~ 15 June to 31 August 2014, and ~~from~~ 1 June to 31 August 2015 ~~in this study~~. There are ~~a total of~~ 11,635 sounding profiles (Fig. 1a) from 19 stations over the TP region consisting of ~~and~~ 47~~57~~45, 2049, and 4841 profiles ~~separately~~ at 08:00 BJT (Fig. 1b), 14:00 BJT (Fig. 1c), and 20:00 BJT (Fig. 1d) , respectively. It is evident that the observational sample size used in this study is much more compared to the previous studies ~~for 19 stations over the TP~~. Meanwhile, it is noted that there is a large difference in the sample ~~number~~ size between the intensive and operational observation records at 08:00 BJT and 20:00 BJT (Fig. 1b and d), which is called the original dataset for convenience. Consequently, ~~Thus~~ we also select the test group dataset which contains the same intensive observation records as the operational ~~observation records~~ ones ~~that correspond to the intensive observation records (called the test group dataset for convenience)~~ at these two times ~~and~~ to make sensitivity ~~repeat the related~~ analyses~~, obtaining the similar results~~ (shown in Section 3.2), which shows that the difference in the sample ~~number~~ size between the intensive and operational observation records does not change our conclusions.

To analyze the factors affecting the ABL in the TP, we use the TIPEX-III 30-min mean surface sensible heat flux (SHF), downward solar radiation, and 5-cm soil volume moisture content at SQH (bare soil with few vegetation~~obstacles~~), Naqu (NQ; alpine steppe), and Linzhi (LZ; alpine meadow with few shrubs and trees) stations in the 2014-2015 summers (Wang et al., 2016; Zhao et al., 2018; Li et al., 2019, 2020). In addition, the manual operational ground-based cloud cover observations ~~observation of total cloudiness (cloud cover)~~ at 02:00 ~~BJT~~, 08:00 ~~BJT~~, 14:00 ~~BJT~~, and 20:00 BJT from the China Meteorological Administration are also used in this study. These ground-based could cover data have been utilized by Guo et al. (2016) and Zhang et al. (2017).

2.2 Calculation method of ABLH

The potential temperature gradient method, proposed by Liu and Liang (2010) and sketched in Fig. 2a, is utilized in identifying the ABL type and calculating the ABL height. The CBL height is defined at the base of the overlying inversion layer that caps the rising convective thermals. The SBL height is defined as the top of the underlying inversion layer, where turbulence decreasing from the surface nearly ceases (Stull 1988). In the evening and morning transition periods when the RL may occur, the neutral RL starting from the ground surface is identified with near-neutral conditions in the surface layer (that is the NBL).

~~We use the potential temperature gradient method proposed by Liu et al. (2010) to calculate the ABL height.~~ Following Liu and Liang ~~et al.~~ (2010), Zhang et al. (2017), and Zhao et al. (2019a), the original sounding observation profiles with a fine vertical resolution of ~1 hPa ~~data~~ are interpolated to ~~new profiles with~~ a vertical resolution of 5 hPa (corresponding to a vertical interval ~~of about~~around 50 m in the ABL) by the nearest neighbor interpolation method~~for the ABL classification and height calculation~~. On the basis of the near-surface thermal gradient, such as a potential temperature (θ) difference (*PTD*) between the fifth layer (~250 m; θ_5) and the second layer (~50 m; θ_2), the ABL is classified as follows.

$$PTD = \theta_5 - \theta_2 \begin{cases} < -\sigma, & \text{for CBL} \\ > +\sigma, & \text{for SBL.} \\ else, & \text{for NBL} \end{cases} \quad (1)$$

Here σ is the stability threshold of the near-surface potential temperature stratification~~a critical value~~. Since the neutral stratification condition (σ = 0) is rare in nature, consistent with Liu and Liang (2010), σ is set to 1.0 K. The threshold value of the NBL is set to -1.0 to 1.0. Consequently, SBLs and CBLs with weak stable or unstable stratification are possibly identified as NBLs.

Once the boundary layer regime has been identified, we use the criteria defined by Liu and Liang (2010) to estimate the ABLH for each regime.~~Consistent with Liu et al. (2010) and Zhang et al. (2017), σ is set to 1.0 K. The ABL height is also calculated on the basis of their methods.~~ Since buoyancy is the dominant mechanism driving turbulence in the CBL~~For both the CBL and NBL~~, the ~~ABL height~~ABLH is ~~calculated~~ defined as the height at which an air parcel rising adiabatically from the surface becomes neutrally buoyant (Stull 1988). First, we find the lowest level (k_1) (Fig. 2a) that meets the following condition

$$\theta_{k_1} - \theta_1 \geq \sigma_u, \quad (2)$$

in which σ_u is the θ increment that represents the minimum strength of the unstable layer. Once level k_1 is determined, another upward scan is performed to find the lowest level at which the potential temperature gradient with height ($\dot{\theta}_k$) meets the following criteria

$$\dot{\theta}_k \equiv \frac{\partial \theta_k}{\partial z} \geq \dot{\theta}_r. \quad (3)$$

Here $\dot{\theta}_r$ is the minimum strength for the overlying inversion layer and can be considered as the overshooting threshold of the rising parcel to define the scope of the entrainment zone for the CBL. The same procedure is adopted to determine the NBL height excluding the entrainment zone at the top (Fig. 2a). Various values of σ_u and $\dot{\theta}_r$ will affect the determination of the boundary layer height and they are respectively set to 0.5 K and 4.0 K km^{-1}, consistent with Liu and Liang (2010). For the SBL, the turbulence in the ABL can result from either buoyancy forcing or wind shear. The SBL height is defined as the lower of the heights of both the thermal stable layer from the surface and the maximum wind ~~shear~~ in the low-level jet stream if present. More details of the definitions of the boundary layer regimes may be seen in Liu and Liang (2010). Figure 2c-d shows the typical profiles of potential temperature for CBL, NBL, and SBL at 20:00 BJT on June 10, 2013, July 21, 2013, and August 11, 2013 at Lasa station, and the ABL heights calculated by the potential temperature gradient method are 3465, 1258, and 409 m AGL, respectively.~~.~~

3 Characteristics of the summer ~~ABL height~~ABLH ~~over~~ in the eastern and western TP

3.1 A general characteristic of the ~~ABL height~~ABLH

The ~~Diurnal~~ diurnal variation is an important feature of the ABL, ~~which~~ consist~~s~~ing of different periods of daytime, night-time, and day/night ~~diurnal~~ transitions ~~(from day to night and from night to day)~~ (Liu and Liang~~et al.~~, 2010). In the central TP (near 90 ℃), 08:00 BJT, 14:00 BJT, and 20:00 BJT correspond to 06:00 (the early morning), 12:00 (noon), and 18:00 (the late afternoon) local solar time (LST)~~standard time~~, respectively. To reveal a difference in ~~the ABL height~~ABLH between the eastern TP (ETP) and the western TP (WTP), we divide all sounding stations ~~over~~ in the TP into two groups. One is for the WTP (to the west of 92.5 ℃) with 8 stations, and the other is for the ETP (to the east of this longitude) with 11 stations.

Figure ~~2a~~3a-c shows the horizontal distribution of the mean ~~ABL height~~ABLH over the TP at 08:00 BJT, 14:00 BJT, and 20:00 BJT, respectively. In the early morning (08:00 BJT), the ABL is of the night-time property. ~~(Fig. 2a), t~~The ~~ABL height~~ABLH is generally low (<450 m AGL) over the TP and displays ~~shows~~ a relatively homogeneous feature(Fig. ~~2~~3a). At this moment, the distribution of the ~~ABL height~~ABLH is narrow, with a frequency peak of 35% at the ~~ABL height~~ABLH of 300 m AGL (Fig. ~~2d~~3d) and 78.5% (99.6%) of the ~~ABL height~~ABLH below 500 ~~m~~ (1000 ~~m~~) m AGL- (Fig. ~~2e~~3e). Figure ~~2f~~ 3f displays the zonal sections of the ~~ABL height~~ABLH along 32 ℃, in which the cross section includes SQH, GZ, SZ, NQ, CD, GanZ, and HY stations. In this figure, the ~~ABL height~~ABLH varies between 218.4 m and 433.9 m from east to west and presents a relatively homogeneous feature in the west-east direction~~, not showing a remarkable west-east difference~~.

At noon (14:00 BJT), with the well developing of the daytime ABL (Fig. 2b3b), the ABLits height remarkably increases over the TP, with an average of 1887.7 m AGL, and exhibits a large west-east difference. There is a wide distribution of the ABL heightABLH up to 4000 m AGL, with a relatively flat peak between 900 m aand 2900 m AGL (Fig. 23d) and only 17.8% (more than 50%) of the ABL heightABLH below 1000 m (above 1900 m) m AGL (Fig. 2e3e). At this moment, tThe regional mean ABL heightABLH is 2124.2 m AGL in the WTP and 1693.5 m AGL in the ETP, with a mean difference of 430.7 m between the WTP and the ETP. Along 32 °N, the ABL heightABLH remarkably increases from 1379.4 m AGL at GanZ station to 2504.2 m AGL at SQH station, with the west-east difference exceeding 1200 m (Fig. 2f3f). This regional difference in the TP ABLH could be likely related to the hydrologic factors such as air moisture and soil water (also see Section 4) that may modulate the spatial distribution of the daytime ABLH (Seidel et al., 2012).

In the late afternoon (20:00 BJT) (Fig. 2c), the ABL begins to turn to the night-time feature. the The ABL heightABLH also starts to decrease in the ETP, with the regional mean height < 1000 m AGL, while it continues to increase at the west-most stationsin the WTP, with the regional mean height > 2000 m AGL (Fig. 3c)., while it begins to decrease in the ETP, with the regional mean height < 1000 m. This result indicates a larger west-east difference of (1054.2 m) between the WTP and the ETP. Especially, the ABL heightABLH is 602 m AGL at HY station and 2920.6 m AGL at SQH station, with a difference above 2000 m between these two stations (Fig. 2f3f). At this moment, the frequency of the high ABL heightABLH decreases., with 12.8% of The the frequency peak is 12.8% at the ABL heightABLH of 300 m AGL (Fig. 2d3d) and 50% of the ABL heightABLHs are less than 1000 m AGL (Fig. 2e3e). It is evident that in daytime the ABL height exhibits an increasing trend from east to west in the TP. Thisthe west-east difference of the ABLH over the TP increases from noon to the late afternoon. After sunset, the daytime boundary layer undergoes a transition to the night-time boundary layer. Since the TP spans almost 1.5 time zones from west to east (15 longitudes equals 1hour time difference), the local solar time is earlier in the west compared to the east, which supports an earlier transition from the daytime ABL to the night-time ABL in the east (Seidel et al., 2010, 2012; Guo et al., 2016).The ABL height reaches the maximum in the late afternoon.

Figure 4 further shows the variations of the ABLH from 08:00 BJT to 14:00 BJT and from 14:00 BJT to 20:00 BJT, indicating varying rates in 6 h. It is seen from Fig. 4a that the ABLH in the TP increases substantially from 08:00 to 14:00 BJT, with a mean growth rate of 1500 m/6 h. There is also a large west-east difference of the ABLH growth rate in this period, with the regional mean of 1800 m/6 h and 1300 m/6 h in the WTP and the ETP, respectively. From 14:00 to 20:00 BJT (Fig. 4b), the growth rate of the ABLH is negative in the ETP, exhibiting an opposite trend to that in Fig. 4a, which indicates a significant decrease (around -600 m/6 h) of the ABLH after noon. In the WTP, the growth rate generally shows a weak increase (around 400 m /6 h) or decrease (around -140 m /6 h). It is evident that the growth rate from 08:00 to 14:00 BJT may indicate the amplitude of the ABL diurnal variation over the TP. Compared to the ETP, the ABL in the WTP has the larger amplitude of the diurnal variation and the longer development time.

3.2 Characteristics of SBL, NBL, and CBL heights

We further examine the characteristics of different ABL types. ~~Figure 3a-c shows the spatial distribution of the SBL height at 00:80 BJT, 14:00 BJT, and 20:00 BJT. It is obvious that the SBL height is generally low and varies between 200 m and 730 m, with a mean height of 336.0 m at 08:00 BJT, 356.0 m at 14:00 BJT, and 321.9 m at 20:00 BJT, not showing a remarkable diurnal variation. For the NBL and CBL, their boundary layer heights are still low in the early morning (Fig. 3d and 3g), with the ABL height < 450 m. In daytime, the NBL and CBL heights remarkably increase, especially in the WTP, with an increasing trend from east to west. At 14:00 BJT (Fig. 3e and 3h), there is a regional mean NBL/CBL height of 2074.6 m/2191.4 m in the WTP and 1594.8 m/1788.0 m in the ETP, with a difference of 479.8 m/403.4 m between the WTP and the ETP. At 20:00 BJT (Fig. 3f and 3i), the NBL/CBL height continues to increase in the WTP, with a regional mean of 2092.0 m/2192.2 m, while the NBL/CBL height decreases in the ETP, with a regional mean of 1423.1 m/1237.2 m. For the NBL and CBL, there are larger differences of 668.9 m and 955.0 m in the ABL height between the WTP and ETP, respectively.~~

Figure ~~4~~ 5 ~~shows~~ presents the spatial distribution of occurrence frequency of SBL, NBL and CBL~~different ABL types~~ at 08:00 BJT, 14:00 BJT, and 20:00 BJT. It is ~~clear~~ seen that the occurrence frequency exhibits ~~shows~~ significant discrepancies at different times~~diurnal variations~~ for the SBL and CBL. At 08:00 BJT, the occurrence frequency of the SBL/CBL is large/little (Fig. ~~4a~~5a/Fig. ~~4g~~5g), with a mean value 84.9%/8.5% over the TP. At 14:00 BJT, the occurrence of the SBL/CBL remarkably decreases/increases, accounting for 3.1%/76.9% of the ABL (Fig. ~~4b~~5b/Fig. ~~4h~~5h). At 20:00 BJT, the SBL/CBL mainly occurs in the ETP/WTP (Fig. ~~4c~~5c/Fig. ~~4i~~5i), with a regional mean of 35.0%/65.0%. ~~This feature is likely related to a difference in the solar elevation angle with respect to longitude because night begins earlier in the WTP than in the ETP, which supports an earlier transition from the daytime CBL to the nighttime SBL in the east (Seidel et al., 2012; Guo et al., 2016).~~However, the NBL shows a relatively weaker temporal ~~diurnal~~ variation over the TP (Fig. ~~4d~~5d-f), with the mean occurrence frequency of 6.4%, 20.0%, and 25.5% at 08:00 BJT, 14:00 BJT, and 20:00 BJT, respectively. The above results are consistent with the diurnal development of the ABL structure including the SBL in the early morning, the CBL at noon, and different types of ABLs between the eastern and western TP in the late afternoon because of the latitudinal difference and the resultant difference in local solar times. Note that the observations were made simultaneously for all stations. Nevertheless, the daytime SBL and the night-time CBL may also occur with low frequencies in the TP, which is likely due to the 'abnormal' forcing associated with certain synoptic conditions or cloud coverage (Medeiros et al., 2005; Poulos et al., 2002; Stull, 1988).

To analyse the temporal variations of the ABLH over the TP, ~~Figure 5 shows~~ the ABL height-occurrence frequency relationships for the SBL, NBL, and CBL at 08:00 BJT, 14:00 BJT, and 20:00 BJT are presented in Fig. 6a-f. For the SBL, the frequency distribution of the ~~ABL height~~ABLH shows the similar feature at three measurement times (Fig. ~~5a~~6a-c) and is

characterized by a narrow single mode, with the frequency peaks of 39.0%, 28.1%, and 36.6% at the ~~ boundary layer height~~ABLH of 200 ~~m~~, 300 ~~m~~, and 300 m AGL at 08:00 ~~BJT~~, 14:00 ~~BJT~~, and 20:00 BJT, respectively, which indicates small temporal variations of the SBL height due to its turbulence inhabited. Moreover, ~~It is found that~~ the SBL height above 80% is < 600 m AGL and the cumulative frequency of the SBL height exceeding 1000 m AGL is little (near zero) at 08:00, 14:00, and 20:00 BJT ~~at these three times~~ (Fig. ~~5d~~6d, e, and f). For ~~The~~ the ~~ABL heights of the~~ NBL and CBL, however, heir heights vary strongly with time under the influence of surface heating in the daytime~~show large variations~~. At 08:00 BJT (Fig. ~~5a~~6a), the distributions of the NBL and CBL heights are narrow, with the frequency peaks of 27.5% and 35.1% at the ~~ABL height~~ABLH of 300 m AGL for NBL and CBL, respectively, similar to that of the SBL, which is possibly due to the initial development of the CBL and NBL in the early morning. At 14:00 BJT ~~(Fig. 5b)~~, the CBL and NBL have ~~there is~~ a wide distribution of the ~~ABL height~~ABLH up to 4000 m AGL, with a relatively flat peak between 1000 ~~m~~ and 3000 m AGL, ~~. This result~~which is remarkably different from a single peak of the SBL. The frequency of the NBL height between 500 and 3000 m AGL is generally less than 5% ~~between 500 m and 3000 m~~ (Fig. ~~5b~~6b), with a frequency peak of 6.1% at 1000 m AGL, and more than 50% NBL height exceeds 1700 m AGL (Fig. ~~5e~~6e). The height of the CBL is higher, with a frequency peak near 4.5% between 1500 ~~m~~ and 2500 m AGL (Fig. ~~5b~~6b). More than 50% CBL height is above 2000 m AGL (Fig. ~~5e~~6e). These results show that the ABL develops well at noon. When the ABL begins turning to the nigh-time property~~This feature is also seen~~ at 20:00 BJT (Fig. ~~5c~~ 6c and ~~5f~~6f),~~.~~ ~~The~~ the distributions of the NBL and CBL heights are still wide but the frequency of the high ~~ABL height~~ABL ~~-~~ height decreases, with the frequency peak below 500 m AGL. It is obvious that the CBL and NBL heights show the similar results consistent with those from Zhang et al (2017). Stull (1998) and Blay-Carreras et al. (2014) revealed that the NBL often occurs in the transition periods between the CBL and the SBL. Since these transitions occur rapidly, the NBL may have the same characteristics in the state variables as the CBL prior to the transition although the dynamic forcing in the NBL maybe weaker compared to the CBL.

To reveal the spatial variations of the ABLH over the TP, the distributions of mean SBL, NBL, and CBL heights at 08:00 BJT, 14:00 BJT, and 20:00 BJT are illustrated in Fig. 7. The SBL height is generally low and varies between 200 and 730 m AGL at these times, with a mean height of 336.0 m AGL at 08:00 BJT, 356.0 m AGL at 14:00 BJT, and 321.9 m AGL at 20:00 BJT (Fig. 7a-c), which indicates the weak spatial differences of the SBL height over the TP at three observation times. For the NBL and CBL, their heights are still low in the early morning (Fig. 7d and 7g), with the ABLH < 450 m AGL, and have small spatial differences. At noon (Fig. 7e and 7h), the NBL and CBL heights rapidly increase, especially in the WTP, which leads to a remarkable east-west gradient in the ABL height. At this moment, there is a regional mean NBL/CBL height of 2074.6/2191.4 m AGL in the WTP and 1594.8/1788.0 m AGL in the ETP, with a difference of 479.8/403.4 m between the WTP and the ETP. In the late afternoon (Fig. 7f and 7i), the NBL/CBL height continues to increase in the WTP, with a regional mean of 2092.0/2192.2 m AGL, while the NBL/CBL height begins decreasing in the ETP, with a regional mean of 1423.1/1237.2 m AGL. This varying feature in the ETP and WTP results in the larger differences of 668.9/955.0 m

in the NBL/CBL height between the WTP and ETP. Thus there is a significant difference in the frequency distribution of the ABL height between the ETP and the WTP in the daytime (Fig. 6g).

~~Because the CBL height shows a remarkable west-east difference in the TP at both 14:00 BJT and 20:00 BJT (shown in Fig. 3h-i), we analyze the cross section of the occurrence frequency of the CBL height along 32 °N for these two times (Fig. 6a), in which the cross section includes SQH, GZ, SZ, NQ, CD, GanZ, and HY stations. In this figure, generally speaking, the high CBL tends to occur more frequently in the WTP than in the ETP. For the ETP, the high frequency of the CBL height mainly occurs below 1400 m, with the peak of 14.4% at the height of 350 m. The occurrence frequency of the CBL height above 2000 m is low (<2%). For the WTP, there are two main peaks of the occurrence frequency. One strong peak (4%-10%) corresponds to the high CBL between 2500 m and 3500 m, especially at SQH station, and another weak peak appears between 200 m and 1000 m. The occurrence frequency is low for the CBL height between 1000 m and 2500 m. Figure 6b shows the cross section of the cumulative occurrence frequency of the CBL height along 32 °N. As illustrated in Fig. 6b, the~~ The cumulative frequency contours gradually go upward from east to west (Fig. 6h). The eastern TP is dominated by a low CBL height, with the peak of 14.4% at the height of 350 m AGL (Fig. 6g) and the ~~the~~ 50% (5%) CBL height below 1000 m AGL (above 2500 m AGL) (Fig. 6h~~,~~). ~~and there is only the 5% CBL height above 2500 m.~~ For the ~~western~~ WTP, the strong peak of 4%-10% corresponds to the high CBL between 2500 and 3500 m AGL (Fig. 6g), especially at SQH station, and there are larger CBL heights, with almost 50% CBL extending upward to more than 2500 m AGL, almost 10% reaching 4000 m AGL or higher, and only 15% CBL below 1000 m AGL (Fig. 6h). ~~The above features indicate a significant difference between the ETP and the WTP in the frequency distribution of the ABL height over the TP.~~

To investigate an effect of differences in the sample profiles shown in Fig. 1b and d, we use the test group dataset to repeat the above analyses. Figures ~~7a~~ 8a and b show the scatter plots of the occurrence frequency of the SBL, NBL, and CBL from the original and test group datasets at each of 19 stations at 08:00 BJT and 20:00 BJT, respectively. It is seen that the correlation coefficients between the two datasets are 0.92-0.99, with root-mean-square errors (RMSEs) of the occurrence frequency between 1.1% and 2.7%. The similar results are also seen in the SBL, NBL, and CBL heights at 08:00 BJT (Fig. ~~7c~~8c) and 20:00 BJT (Fig. ~~7d~~8d). The correlation coefficients in the ABL height are 0.90-0.99. The RMSE of the SBL height is 14 m and 25 m at 08:00 and 20:00 BJT, respectively. The RMSE of the CBL and NBL heights are 54-59 m at 08:00 BJT and 99-107m at 20:00 BJT. These high correlations and little errors show that the difference in the sample number does not change our conclusions.

From the foregoing analysis, the CBL and NBL heights ~~the ABL height~~ in the TP show~~s a~~ remarkable temporal~~d diurnal~~ variations and west-east spatial differences, while these features are not remarkable for the SBL~~especially for both NBL and CBL~~. From noon to the late afternoon, the NBL and CBL are deeper ~~there are larger NBL and CBL heights~~ in the WTP compared to the ETP, with the differences between the WTP and the ETP exceeding 600 m AGL ~~of 668.9 m and 955.0 m between the WTP and the ETP~~ at 20:00 BJT~~, respectively~~. Then, which factors contribute to ~~these~~ this difference~~s~~ in the

ABL between the WTP and ETP? In the following section, we examine some factors that may be responsible for ~~to~~ the ABL height over the TP.

4 Factors responsible for the ABL height over the TP

Previous ~~A lot of~~ studies have addressed effects of surface sensible heat flux (SHF), soil volume moisture content (VWC), downward solar radiation flux (DSR), and the ~~total~~ cloud cover (CLD) on ABL height (Lilly, 1964; Liu, et al., 2004; Brooks and Rogers, 2006; Zhao et al., 2011; Sanchez-Mejia and Papuga, 2014; Rihani et al., 2015; Lin et al., 2016; Zhang et al., 2017; Zhang et al., 2019; Qiao et al., 2019). However, these studies paid little attention to reasons for the west-east difference of the ABL between the eastern and western TP. To investigate a possible reason for ~~the~~ this difference ~~in the ABL height between the eastern and western TP~~, we utilize the TIPEX-III SHF, DSR, and VWC ~~and CLD observations~~ at SQH, NQ, and LZ stations, and the corresponding meteorological operational CLD observations to ~~analyzing~~ analyze the relationships between the above variables and the ABL height.

The driving force of turbulence in the ABL is the surface buoyancy flux as a result of surface and air temperature and humidity differences and the mean surface layer wind. The kinematic heat flux (KHF) and kinematic moisture flux (KMF) at the surface are the two directly factors responsible for the surface buoyancy flux (Brooks and Rogers, 2006). Since KMF is often small, KHF associated with SHF is examined as a major component of buoyancy flux in dry conditions over land. According to the method of Brooks and Rogers (2006), our calculation results show that the contribution from KMF to surface buoyancy flux is below 18% at SQH, NQ, and LZ stations. Moreover, the ABL may be largely affected by the effect of cumulative SHF in the daytime (Zhang et al., 2019). Thus we analyse the possible effect of SHF on the ABL. Figure ~~8a~~9a-c ~~shows~~ presents the scatter plots between the mean SHF over the past six hours~~the 6-hour mean SHF~~ and the ABL height at SQH, NQ, and LZ stations. As shown in this figure, the correlation is 0.80, 081, and 0.71 (significant at the 99% confidence level) at these ~~the three~~ stations, respectively. ~~That is, w~~When SHF is strong, the turbulent motion is strong and the ~~ABL height~~ABL develops, which is consistent with the~~supports the~~ result of Zhang et al. (2011b). Their result shows a significant correlation of 0.78 in the arid area of Northwest China between the ABL thickness and the cumulative SHF. Figures ~~9a~~ 10a and b further present the features of the ABL height and SHF at SQH, NQ, and LZ stations. The ~~maximum~~ mean value of SHF is ~~270~~ 85 W/m^2, ~~165~~ 42 W/m^2, and ~~100~~ 33 W/m^2 at SQH, NQ and GZ stations, respectively, and has a large difference (~~105~~ 52 W/m^2) between SQH and NQ stations. This result indicates a decreasing trend of SHF from west to east in the TP, consistent with a reduction of the ABL height from SQH via NQ to LZ station (shown in Figs. 3 and ~~9a~~10a). In addition, Fig. ~~10~~ 11 demonstrates the diurnal variations of SHF and the ABL height at SQH, NQ, and LZ stations. The duration of positive SHF in a diurnal cycle at SQH, NQ and GZ stations is 14, 12 and 11 hours, respectively, and indicates a decreasing trend from west to east in the TP. It is clear that the peak of the SHF ~~diurnal variation~~ occurs earlier ~~compared~~ than the maximum~~to that of the~~ ABLH in a diurnal cycle ~~height~~ at SQH station. The maximum ABL height occurs near 20:00 BJT

(approximately 17:20 LST), corresponding to a stronger SHF. At LZ station, however, the SHF turns into a negative value at 20:00 BJT (18:20 LST) and then the ABL height decreases~~the ABL height at 20:00 BJT (18:20 LST) corresponds to a negative SHF~~. ~~This difference in SHF between SQH and LZ stations is possibly associated with more cloud cover (reducing the solar radiance at the surface) and one-hour time difference (an earlier transition to night at LZ station).~~ Some past studies show that the development of ABL height generally lags the development of SHF, and ABL depth growth continues even after SHF attains the maximum daytime value until the time of early evening transitions (Chen et al., 2016; Zhang et al., 2019). Consequently, the difference in the ABL height between the WTP and ETP is closely associated with~~may be attributed to~~ a west-east difference in SHF that is as a direct thermal factor ~~affecting~~ for the ABL development in the TP.

The solar radiation at the surface is an important component of the surface energy budget, affecting ~~land~~ surface temperature and SHF. We show the scatter plots between the 6-hour mean DSR and the ABL height at SQH, NQ, and LZ stations (Fig. ~~8d~~9d-f). The ABL height is highly correlated with the 6-hour average of DSR at these stations, with the correlation coefficients of 0.86, 081, and 0.73, respectively, which is equivalent to those of SHF. The mean DSR shows a decreasing trend from SQH (510 W/m^2) to LZ (200 W/m^2) station. Since the solar irradiance at the surface is negatively associated with the local cloud cover (Guo et al., 2011; Lin et al., 2016; Li et al., 2017; Zhang et al., 2017), the cloud cover is also correlated to the ABL height. Figure ~~8g~~9g-i show that the 6-hour mean CLD has significant correlations of -0.56, -0.65, and -0.54 with the ABL height at SQH, NQ, and LZ stations, respectively. A decrease of the mean ABL height from SQH to LZ station (Fig. ~~9a~~10a) is corresponded to an increase of cloud cover (Fig. ~~9d~~10d) and a decrease of DSR (Fig. ~~9e~~10c). When cloud cover is between 0 and 20%, the mean ABL height for the NBL and CBL is 2019 m AGL~~.~~/2732 m AGL in the ETP/WTP and when cloud cover is >80%, the ABL height decreases to 741 m AGL~~.~~/1626 m AGL in the ETP/WTP (Fig. ~~11~~12). Therefore, the increased cloud cover inhibits the development of both the NBL and CBL. The difference in cloud cover between the WTP and ETP contributes to the west-east distribution of DSR and SHF, also finally contributing to the difference of the ABL development. Corresponding to more cloud cover in the ETP, the local ABL is more closely associated with atmospheric moisture processes.

Soil moisture is also an important factor affecting SHF. Low soil moisture generally coincides with a high surface sensible heat flux, which facilitates the ABL development (e.g., McCumber and Pielke, 1981; Sanchez-Mejia and Papuga, 2014; Rihani et al., 2015). Figure ~~8j~~9j-l shows that the relationship between the ABL height and the 6-hour mean VWC at SQH, NQ, and LZ stations. The ABL height at LZ station is negatively correlated to the local soil moisture, with a significant correlation coefficient of -0.45~~,~~. ~~which~~ This result indicates that the ABL height is lower when surface soil is moister. However, the negative correlation is weaker at SQH station, with a correlation coefficient of -0.21. This difference between the WTP and the ETP ~~is~~ may be associated with the climatic feature of the local soil moisture. The surface type transitions from alpine meadow with few shrubs and trees or alpine steppe in the ETP to bare soil with few obstacles in the WTP (Lin et al., 1981; Wang et al., 2016). Accordingly, soil moisture decreases gradually from the ETP to the WTP (Fig. ~~9e~~10e), with a

mean value of soil moisture below 0.10 m^3/m^3 at SQH station and 0.38 m^3/m^3 at LZ station. Little soil moisture in the WTP has a weak modulation to the local surface heat flux, which ~~results in~~may lead to a weak correlation between the ABL height and soil moisture in the WTP.

5 Summary and discussion

Using the summer TIPEX-III intensive and meteorological operational observational datasets, we examine the ABL features and the relationships of the ABL height with surface sensible heat flux, solar radiation, cloud cover, and soil moisture in the TP region. The main conclusions are summarized as follows.

Generally speaking, ~~The~~ the ABL height exhibits diurnal variations and regional differences in the TP, especially for the CBL and NBL. These features ~~which~~ are weak for the SBL ~~and remarkable for both NBL and CBL~~. Compared to the ETP, the ABL in the WTP has the larger amplitude of the diurnal variation and the longer development time. In the early morning, the ABL height is generally low over the TP, not showing a large west-east difference, and the distribution of the ABL height is narrow, with 78.5% of the ABL height < 500 m AGL. At noon, the CBL and NBL heights remarkably increase and have a wide distribution in the ABL height up to 4000 m AGL, with more than 50% of the ABL height exceeding 1900 m AGL. ~~The~~ Their height~~s~~ exhibit~~s~~ a large west-east difference. At this moment, the distribution of the SBL height is also narrow, with the cumulative frequency of 80% at the height of 500 m AGL, and there is no remarkable ~~the~~ west-east difference ~~is not obvious~~. In the late afternoon, there are a narrow distribution of the SBL height and wide distributions ~~ones~~ of both the NBL and CBL heights. At this moment, ~~The~~ the ABL height continues to increase in the WTP, while it begins to decrease in the ETP. This feature results in a larger west-east difference in the ABL height. In spite of a cold environment in the TP (relative to plain areas), the WTP still has the ABL height above 2000 m AGL, which is similar to some extreme hot and arid areas such as Dunhuang and Taklimakan Deserts. In the ETP, the ABLH is similar to that in North China (1500-1900 m AGL) and is generally larger compared to the East Asian summer monsoon region (＜1500 m AGL) such as the Yangtze River Delta and the Pearl River Delta (Zhang et al., 2011; Guo et al., 2016; Zhang et al., 2017; Qiao et al., 2019).

The occurrence frequency ~~For~~ of the SBL and CBL in the TP ~~, the occurrence frequency~~ shows remarkable ~~diurnal~~ temporal variations. Most (few) of the SBLs (CBLs) ~~in the TP~~ occur in the early morning and ~~its~~ the occurrence frequency rapidly decreases (increases) at noon, accounting for 3.6% (76.9%) of the ABL in the TP. ~~Moreover, p~~Possibly ~~due~~ owing to a difference in the solar elevation angle with respect to longitude in the late afternoon, the SBL and CBL dominate~~s~~ the ETP and WTP, respectively. However, the NBL shows a relatively weak ~~diurnal~~ temporal variation over the TP, with the mean occurrence frequency of 6.4% in the early morning and around 20% at noon and in the late afternoon.

The ABL height is significantly correlated to SHF, DSR, and cloud cover in the TP and is also closely associated with~~to~~ soil moisture in the ETP. The decreasing trends in both SHF and DSR and the increasing trends in both cloud cover and soil moisture from west to east may cause the corresponding ~~The~~ west-east reduction in the ABL height ~~is closely associated with the decreasing trends in both SHF and DSR and the increasing trends in both cloud cover and soil moisture from west to east~~. ~~The above factors affecting the WET and ETP ABL heights are summarized in Fig. 12.~~ ~~That is, i~~In the WTP (ETP), with low (high) cloud cover, there is larger (smaller) downward solar radiation at the surface. Meanwhile, corresponding to bare soil (alpine meadow or steppe) in the WTP (ETP), there is a dry (wet) soil condition. These features cause high (low) sensible heat flux, thus promoting (inhibiting) the local ABL development. The above factors affecting the WET and ETP ABL heights are summarized in Fig. 1~~2~~3.

The Tibetan Plateau is an area very sensitive to global climate change, which exerts important thermal and dynamical effects on the general circulation and climate through the unique and complex land surface and boundary layer processes. Owing to new sounding observations in the WTP, our analysis firstly reveals remarkable west-east differences in the ABL height, occurrence frequency, and diurnal amplitude over the TP region during summer. It is noted that there is a big drop in the CBL height from 3000–4000 m AGL to 1000–2000 m AGL from the WTP to the ETP~~the peak ABL height can drop from 3000–4000 m for a deep CBL in the WTP to 1000–2000 m for a shallow CBL in the ETP~~. Such a steep west-east inhomogeneity in the TP (with an East-West spatial scale of about 2000 km) is remarkably different from the regional variability of the ABLH on much larger scales (~4000 km) such as in the United States (Seidel et al., 2012) and in China (Guo et- al., 2016). This unique inhomogeneity in the TP ~~inhomogeneous distribution of the ABL height~~ may trigger local mesoscale circulation and precipitation (Segal et al., 1992; Goutorbe et al., 1997; Huang et al., 2009; Zhang et al., 2019; Qiao et al., 2019). Therefore, the influences of west-east differences in the ABLH ~~height~~ over the TP on the local weather and climate should be further studied in the future. In addition, this study merely investigates the characteristics of the summer ABLH in TP due to the limitation of the intensive sounding observations. More efforts should be made to expand the climatology of ABLH to other seasons in TP when more sounding data are available.

Code and data availability. All data used are available from the TIPEX-III ~~for providing the data available~~ on its homepages (http://data.cma.cn/tipex).

Author contributions. J.C. designed the study, analyzed the data and wrote the manuscript. P.Z. contributed to the study design and writing of the manuscript.

Competing interests. The authors declare that they have no conflict of interest.

Acknowledgements. We thank the TIPEX-III for providing the data available on its homepages (http://data.cma.cn/tipex). This work is supported by the National Key Research and Development Program of China and the Strategic Priority Research Program of Chinese Academy of Sciences.

Financial support. This work is jointly funded by the National Key Research and Development Program of China (Grant 2018YFC1505700) and the Strategic Priority Research Program of Chinese Academy of Sciences (XDA20100300).

References

Blay-Carreras, E., Pino, D., Vil à-Guerau de Arellano, J., van de Boer, A., De Coster, O., Darbieu, C., Hartogensis, O., Lohou, F., Lothon, M., Pietersen, H.: Role of the residual layer and large-scale subsidence on the development and evolution of the convective boundary layer, Atmos. Chem. Phys., 14, 4515-4530, doi:10.5194/acp-14-4515-2014, 2014.

Bosveld, F. C., and Coauthors: The third GABLS intercomparison case for evaluation studies of boundary-layer models. Part B: Results and process understanding, Bound.-Layer Meteor., 152, 157–187, doi:10.1007/s10546-014-9919-1, 2014.

Brooks, I. M., Rogers, D. P.: Aircraft observations of the mean and turbulent structure of a shallow boundary layer over the Persian Gulf, Bound.-Layer Meteor., 95, 189-210, doi:10.1023/A:1002623712237, 2000.

Chen, S. S., and Houze, R. A.: Diurnal variation and life-cycle of deep convective systems over the tropical Pacific warm pool, Quart. J. Roy. Meteor. Soc., 123, 357–388, doi:10.1002/qj.49712353806, 1997.

Chen, X. L., Juan, A. Añel., Su, Z. B., Laura, de. La. Torre., Hennie, Kelder., Jacob, van. Peet., Ma, Y. M.: The deep atmospheric boundary layer and its significance to the stratosphere and troposphere exchange over the Tibetan Plateau, PLoS. ONE, 8, e56909, doi:10.1371/journal.pone.0056909, 2013.

Chen, X. L., Škerlak, B., Rotach, M. W., Juan, A. Anel., Su, Z. B., Ma, Y. M., Li, M. S.: Reasons for the extremely high-ranging planetary boundary layer over the Western Tibetan Plateau in winter, J. Atmos. Sci., 73, 2021-2038, doi:10.1175/jas-d-15-0148.1, 2016.

Dai, C., Wang, Q., Kalogiros, J. A., Lenschow, D. H., Gao,Z., Zhou, M.: Determining boundary-layer height from aircraft measurements, Bound.-Layer Meteor., 152, 277–302, doi:10.1007/s10546-014-9929-z, 2014.

Davy, R., and Esau, I.: Differences in the efficacy of climate forcings explained by variations in atmospheric boundary layer depth, Nat. Commun., 7, 11690, doi:10.1038/ncomms11690, 2016.

Davy, R.: The climatology of the atmospheric boundary layer in contemporary global climate models, J. Climate, doi:10.1175/JCLI-D-17-0498.1, 2018.

Driedonks, A. G. M. and Tennekes, H.: Entrainment effects in the well-mixed atmospheric boundary layer, Bound.-Layer Meteor., 30, 75-105, doi:10.1007/BF00121950, 1984.

Esau, I., and Zilitinkevich, S.: On the role of the planetary boundary layer depth in the climate system, Adv. Sci. Res., 4, 63–69, doi:10.5194/asr-4-63-2010, 2010.

Garratt, J. R.: The Atmospheric Boundary Layer, Cambridge, Univ. Press., 37, 89-134, doi:10.1007/3-211-38078-7_4, 1992.

Garratt, J. R.: Sensitivity of climate simulations to land-surface and atmospheric boundary-layer treatments—A review, J. Climate, 6, 419–448, doi:10.1175/1520-0442(1993)006<0419:socstl>2.0.co;2, 1993.

Goutorbe, J. P., Lebel, T., Dolman, A. J., Gash, J. H. C., Kabat, P., Kerr, Y. H., Monteny, B., Prince, S. D., Stricker, J. N. M., Tinga, A., Wallace, J. S.: An overview of HAPEX-Sahel: A study in climate and desertification, J. Hydrol., 188-189, 4-17, doi:10.1016/S0022-1694(96) 03308-2, 1997.

Guo, J. P., Zhang, X. Y., Che, H. Z., Gong, S. L., An, X., Cao, C. X.: Correlation between PM concentrations and aerosol optical depth in eastern China, Atmos. Environ., 43, 5876-5886, doi:10.1016/j.atmosenv.2009.08. 026, 2009.

Guo, J. P., Miao, Y. C., Zhang, Y., Liu, H., Li, Z. Q., Zhang, W. C., He, J., Lou, M. Y., Yan, Y., Bian, L. G., Zhai, P. M.: The climatology of planetary boundary layer height in China derived from radiosonde and reanalysis data, Atmos. Chem. Phys., 16, 13309-13319, doi:10.5194/acp-16-13309-2016, 2016.

Holtslag, B. and Boville, B. A.: Local versus nonlocal boundary-layer diffusion in a global climate model. J. Climate, 6, 1825–1842, doi:10.1175/1520-0442(1993)0062.0.CO;2,1993.

Hong, J., Guo, J., Du, J., Wang, P.: An observational study on the vertical structure of the upper troposphere and lower stratosphere in Gaize, Tibet during the rainy season, Acta Meteor. Sinica, 74, 827-836, doi:10.11676/qxxb2016.05, 2016.

Huang, J. P., Minnis, P., Yi, Y., Tang, Q., Wang, X., Hu, Y., Liu, Z., Ayers, K., Trepte, C., Winker, D.: Summer dust aerosols detected from CALIPSO over the Tibetan Plateau, Geophys. Res. Lett., 34, L18805, doi:10.1029/2007GL029938, 2007.

Huang, Q., Marsham, J. H., Parker, D. J., Tian, W., Weckwerth, T.: A comparision of roll and nonroll convection and the subsequent deepening moist convection: An LEM case study based on SCMS data, Mon. Wea. Rev., 137, 350-365, doi:10.1175/2008MWR2450.1, 2009.

Li, J. L., Hong, Z. X., Sun, S. F.: An observational experiment on the atmospheric boundary layer in Gerze area of the Tibetan Plateau, Chinese J. Atmos. Sci., 24, 301-312, doi:10.3878/j.issn.1006-9895.2000.03.02, 2000.

Li, Y., Gao, W.: Atmospheric boundary layer circulation on the eastern edge of the Tibetan Plateau, China, in summer, Arct. Antarct. Alp. Res., 39, 708-713, doi:10.1657/1523-0430(07-50 4)[li]2.0.co;2, 2007.

Li, M. S., Ma, Y. M., Ma, W. Q., Ishikawa, Hirohiko., Sun, F. L., Ogino, S. Y.: Structural difference of atmospheric boundary layer between dry and rainy seasons over the central Tibetan Plateau, Journal of Glaciology and Geocryology, 33, 72-79, doi:10.3724/SP.J.1146.2006.01085, 2011.

Li, Z., Guo, J., Ding, A., Liao, H., Liu, J., Sun, Y.: Aerosol and boundary-layer interactions and impact on air quality, Natl. Sci. Rev., 4, 810-833, doi:10.1093/nsr/nwx117, 2017.

Li, N., Zhao, P., Wang, J., Deng, Y.: Estimation of surface heat fluxes over the central Tibetan Plateau using the maximum entropy production model, J. Geophys. Res.-Atmos., 124, 6827–6840, doi:10.1029/2018JD029959, 2019.

Li, N., Zhao, P., Wang, J., Deng, Y.: The Long-Term Change of Latent Heat Flux over the Western Tibetan Plateau. Atmosphere, 11, 262, doi:10.3390/atmos11030262, 2020.

Lin, Y., Wang, Y., Zhang, R., Liu, Y.: Response of boundary layer clouds to continental pollution during the RACORO campaign, J. Atmos. Sci., 73, 3681–3700, doi:10.1175/JAS-D-15-0361.1, 2016.

Liu, S. H., Xu, Y., Hu, F.: Using a Modified Soil-Plant-Atmosphere Scheme (MSPAS) to simulate the interaction between land surface processes and atmospheric boundary layer in semi-arid regions, Adv. Atmos. Sci., 21(2): 245-259, doi:10.1007/bf029157 11, 2004.

Liu, S. Y., Liang, X. Z.: Observed diurnal cycle climatology of planetary boundary layer height, J. Climate, 23, 5790-5809, doi:10.1175/2010JCLI3552.1, 2010.

Liu, H. Y., Miao, M. Q.: Preliminary analysis on characteristics of boundary layer in Qinghai-Tibet Plateau, Journal of Nanjing University (Natural Sciences), 37, 348-357, doi:10.3321/j.issn:0469-5097.2001.03.013, 2001.

Lü, Y. Q., Ma, Y. M., Li, M. S., Sun, F. L.: Study on characteristic of atmospheric boundary layer over Lake Namco region, Tibetan Plateau, Plateau Meteor., 27, 1205-1210, doi:ir.casnw.net/handle/362004/9294, 2008.

McCumber, M. C., and Pielke, R. A.: Simulation of the effects of surface fluxes of heat and moisture in a mesoscale numerical model: 1. Soil layer, J. Geophys. Res., 86, 9929-9938, doi:10.1029/JC086iC10p09929, 1981.

Miao, Y. C., Hu, X. M., Liu, S. H., Qian, T. T., Xue, M., Zheng, Y. J., Wang, S.: Seasonal variation of local atmospheric circulations and boundary layer structure in the Beijing-Tianjin-Hebei region and implications for air quality, J. Adv. Model. Earth Syst., 7, 1602-1626, doi:10.1002/2015MS000 522, 2015.

Pal, S., and Haeffelin, M.: Forcing mechanisms governing diurnal, seasonal, and interannual variability in the boundary layer depths: Five years of continuous lidar observations over a suburban site near Paris, J. Geophys. Res. Atmos., 120, 11936-11956, doi: 10.1002/2015JD023268, 2015.

Qiao, L., Zhang, Q., Yue, P., et al.: Analysis of changes in the structure of atmospheric boundary layer from non-monsoon zone to monsoon zone, Chinese J. Atmos. Sci., 43 (2): 251-265, doi:10.3878/j.issn.1006-9895.1805.17231, 2019.

Raman, S., Templeman, B., Templeman, S., Holt, T., Murthy, A. B., Singh, M. P., Agarwaal, P., Nigam, S., Prabhu, A., Ameenullah, S.: Structure of the Indian southwesterly pre-monsoon and monsoon boundary layers: Observations and numerical simulation, Atmos. Environ., 24, 723-734, doi:10.1016/0960-1686(90)90273-p, 1990.

Rihani, J. F., Chow, F. K., Maxwell, R. M.: Isolating effects of terrain and soil moisture heterogeneity on the atmospheric boundary layer: Idealized simulations to diagnose land atmosphere feedbacks, J. Adv. Model. Earth Syst., 7, 915-937, doi:10.1 002/2014MS000371, 2015.

Sanchez-Mejia, Z. M., and Papug, S. A.: Observations of a two-layer soil moisture influence on surface energy dynamics and planetary boundary layer characteristics in a semiarid shrubland, Water Resour. Res., 50, 306-317, doi:10.1002/2013 WR014135, 2014.

Segal, M., Arritt, R. W.: Nonclassical mesoscale circulations caused by surface sensible heat-flux gradients, Bull. Amer. Meteor. Soc., 73, 1593-1604, doi:10.1175/1520-0477(1992) 0732.0.CO;2, 1992.

Seibert, P., Beyrich, F., Gryning, S. E., Joffre, S., Rasmussen, A.,Tercier, P.: Review and intercomparison of operational methods for the determination of the mixing height, Atmos. Environ., 34, 1001-1027, doi:10.1016/s1352-2310(99)00349-0, 2000.

Seidel, D. J., Ao, C. O., Li, K.: Estimating climatological planetary boundary layer heights from radiosonde observations: Comparison of methods and uncertainty analysis, J. Geophys. Res.-Atmos., 115, D16113, doi:10.1016/s1352-2310(99)00349-0, 2010.

Seidel, D. J., Zhang, Y., Beljaars, A., Golaz, J.-C.,Jacobson, A. R.,Medeiros, B.: Climatology of the planetary boundary layer over the continental United States and Europe, J. Geophys. Res.-Atmos., 117, D17106, doi:10.1029/2012jd018143, 2012.

Song, Z. S., Zhu, B., Sun, G. W.: A preliminary study on the thermal mixing layer in the western Tibetan Plateau, the Collected Works of the Tibetan Plateau Meteorological Scientific Experiment (Series 2), Beijing: Science Press, 253-261, 1984.

Stull, R. B.: An Introduction to Boundary Layer Meteorology, Springer Netherlands, doi:10.1007/978-94-009-3027-8, 1988.

Sun, F., Ma, Y., Li, M.: Boundary layer effects above a Himalayan valley near Mount Everest, Geophys. Res. Lett., 34, L08808, doi:10.1029/2007gl029484, 2007.

Tao, S. Y., Ding, Y. H.: Observational evidence of the influence of the Qinghai-Xizang (Tibet) Plateau on the occurrence of heavy rain and severe convective storms in China, Bull. Amer. Meteor. Soc., 62, 23-30, doi:10.1175/1520-0477(1981)062h0023:OEOTIOi2.0.CO;2, 1981.

Wang, Y. J., Xu, X. D., Liu, H. Z., Li, Y. Q., Li, Y. H., Hu, Z. Y., Gao, X. Q., Ma, Y. M., Sun, J. H., Lenschow, D. H., Zhong, S. Y., Zhou, M. Y., Bian, X. D., Zhao, P., Wang, Y. J.: Analysis of land surface parameters and turbulence characteristics over the Tibetan Plateau and surrounding region, J. Geophys. Res. Atmos., 121, 9540-9560, doi:10.1002/2016JD025401, 2016.

Xu, X., Bian, L., Zhang, G., Bian, L. G., Zhang, G. Z., Liu, H. Z.: A comprehensive physical pattern of land-air dynamic and thermal structure on the Qinghai-Xizang Plateau, Science in China Series D: Earth Sciences, 45, 577-594, doi:10.1360/02yd9060, 2002.

Yanai, M., Li, C.: Mechanism of heating and the boundary layer over the Tibetan Plateau, Mon. Wea. Rev., 122, 305-323, doi:10.1175/1520-0493(1994)1222.0.CO;2, 1994.

Yang, K., Koike, T., Fujii, H., Tamura, T., Xu, X., Bian, L., Zhou, M. Y.: The daytime evolution of the atmospheric boundary layer and convection over the Tibetan Plateau: observations and simulations, J. Meteor. Soc. Japan, 82, 1777-1792, doi:10.2151/jmsj.82.1777, 2004.

Ye, D., Gao, Y. X.: The Meteorology of the Qinghai-Xizang Plateau, Beijing: Science Press, 89-101, 1979.

Yu, X. J., Du, J., Wang, M. Z., Xu, H. X., He, Q.: Impact of assimilating the new radiosonde data on Qinghai-Tibetan Plateau on summer rainfall forecast over southern Xinjiang, Plateau Meteor., 37(1), 13-27, doi:10.7522/j.issn.1000-0534.2017.00034, 2018.

Zhang, G., Xu, X., Wang, J.: A dynamic study of Ekman characteristics by using 1998 SCSMEX and TIPEX boundary layer data, Adv. Atmos. Sci., 20, 349-356, doi:10.1007/bf02690793, 2003.

Zhang, Y., Seidel, D. J., Golaz, J.-C., Deser, C.,Tomas, R. A.: Climatological characteristics of Arctic and Antarctic surface-based inversions, J. Climate., 24, 5167-5186, doi:10.1 175 /2011JCLI4004.1, 2011a.

Zhang, Q., Zhang, J., Qiao, J., Wang, S.: Relationship of atmospheric boundary layer depth with thermodynamic processes at the land surface in arid regions of China, Sci. China: Earth Sci., 54, 1586-1594, doi:10.1007/s11430-011-4207-0, 2011b.

Zhang, Q., Yue, P., Zhang, L., et al.: Land-atmosphere interaction over the summer monsoon transition zone in China: A review and prospects, Acta Meteor. Sinica, 77, 758-773, 2019.

Zhang, W., Guo, J., Miao, Y., Liu, H., Yang, S., Fang, Z., He, J., Lou, M. Y., Yan, Y., Li, Y., Zhai, P. M.: On the summertime planetary boundary layer with different thermodynamic stability in China: a radiosonde perspective, J. Climate, 31, doi:10.1175/jcli-d-17-0231.1, 2017.

Zhao, C. L.， Li, Y. H., Liu, Y. P., et al.: The variation characteristics of planetary boundary layer height in Northwest China: Based on radiosonde and ERA-Interim reanalysis data, Plateau Meteor., 38, 1181-1193, doi:10.7522 /jissn.100005 34.2018. 00152, 2019a.

Zhao, J. H., Zhang, Q., Wang, S.: A simulative study of the thermal mechanism for development of the convective boundary layer in the arid zone of Northwest China, Acta Meteor. Sinica, 69, 1029-1037, doi:10.11676/qxxb2011.090, 2011.

Zhao, M., Miao, M. Q.: The atmospheric boundary layer, Beijing: China Meteorological Press, 1992.

Zhao, P., Xu, X., Chen, F., et al.: The Third Atmospheric Scientific Experiment for understanding the earth–atmosphere coupled system over the Tibetan Plateau and its effects, Bull. Amer. Meteor. Soc., 99, 757-776, doi:10.1175/BAMS-D-16-0050.1, 2018.

Zhao, P., Li, Y. Q., Guo, X. L., et al.: The Tibetan Plateau surface-atmosphere coupling system and its weather and climate effects: The Third Tibetan Plateau Atmospheric Science Experiment, J. Meteor. Res., 33, 375-399, doi:10.1007/s13351-019-8602-3, 2019b.

Zhou, W., Yang, S. P., Jiang, X., et al: Estimating planetary boundary layer height over the Tibetan Plateau using COSMIC radio occultation data, Acta Meteor. Sinica, 76, 117-133, doi:10.11676/qxxb2017.069, 2018.

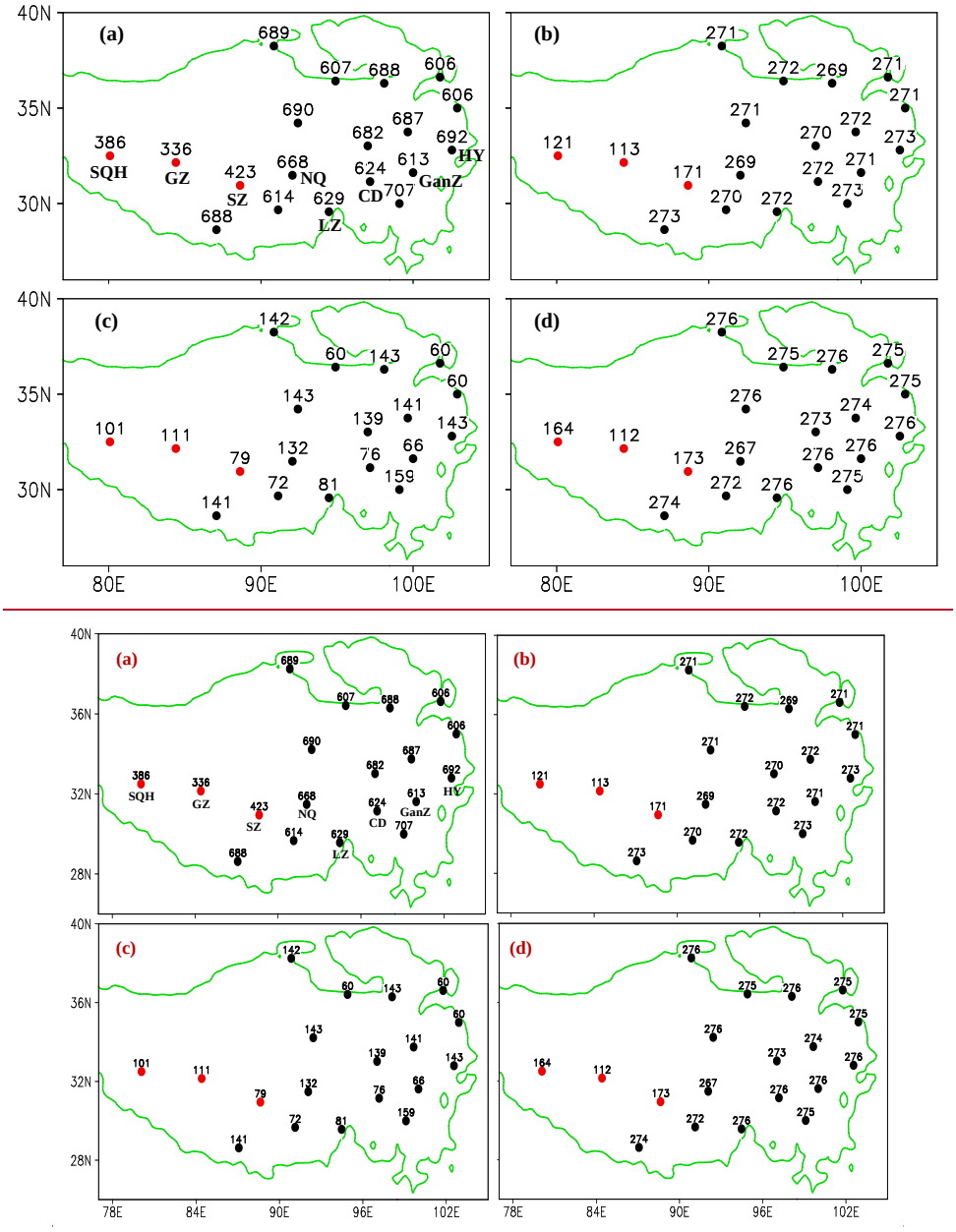

Figure 1: Distribution of sounding stations, in which the number indicates sounding profiles at each station at (a) 08:00, 14:00, and 20:00 BJT,~~all times,~~ (b) 08:00 BJT, (c) 14:00 BJT, and (d) 20:00 BJT in the study period. Red (black) dots represent intensive (operational) observations~~sites~~. Some observation station names are given as abbreviations in (a) and the green line shows the 3000 m topography~~Some letters are for the abbreviated names of stations. The green line is for the topography above 3 km~~.

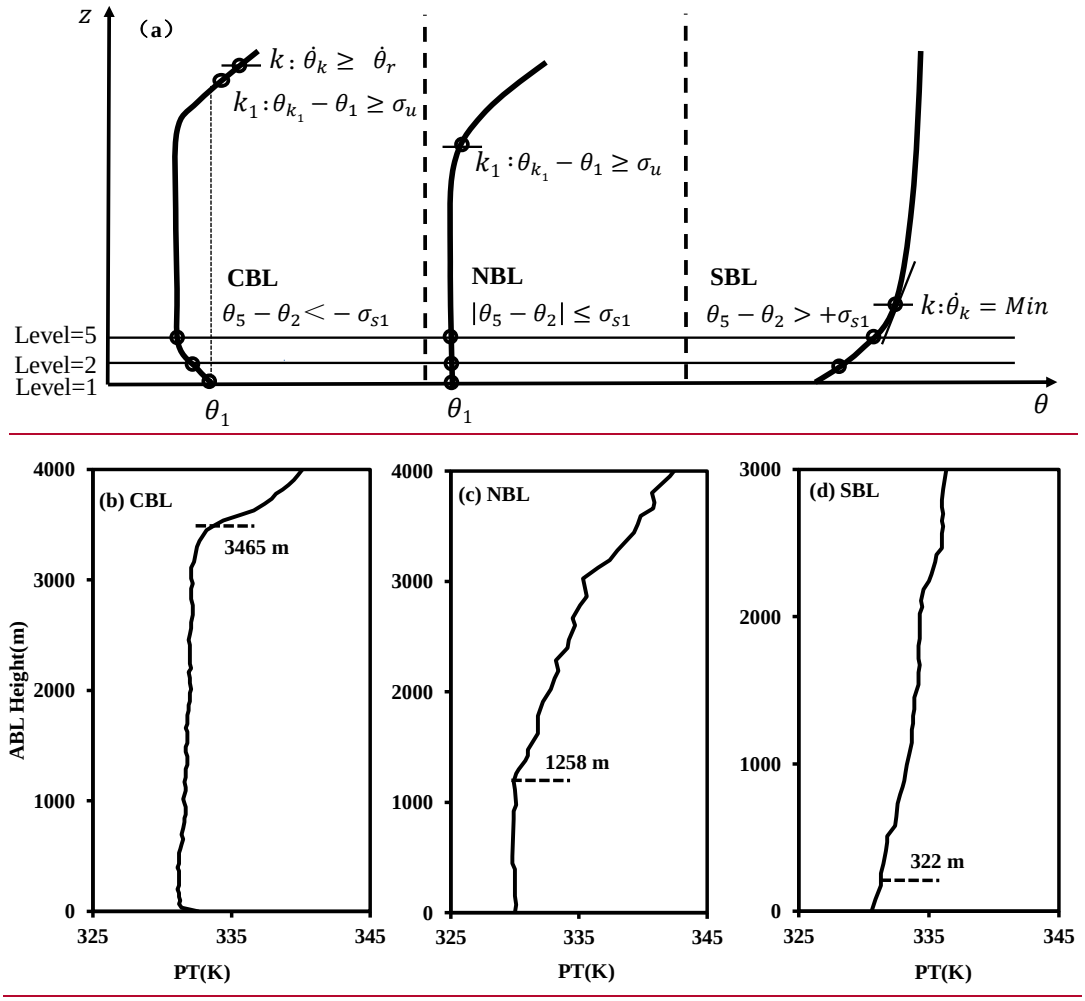

Figure 2: (a) Illustration of the determination procedure for the convective boundary layer (CBL), neutral boundary layer (NBL), and stable boundary layer (SBL) heights; and examples of the potential temperature (PT) profiles derived from sounding observation at Lasa station at 20:00 BJT for (b) CBL on June 10, 2013, (c) NBL on July 21, 2013, and (d) SBL on August 11, 2013, respectively. The dash line in (b)-(d) represents the ABL height identified using the algorithm described.

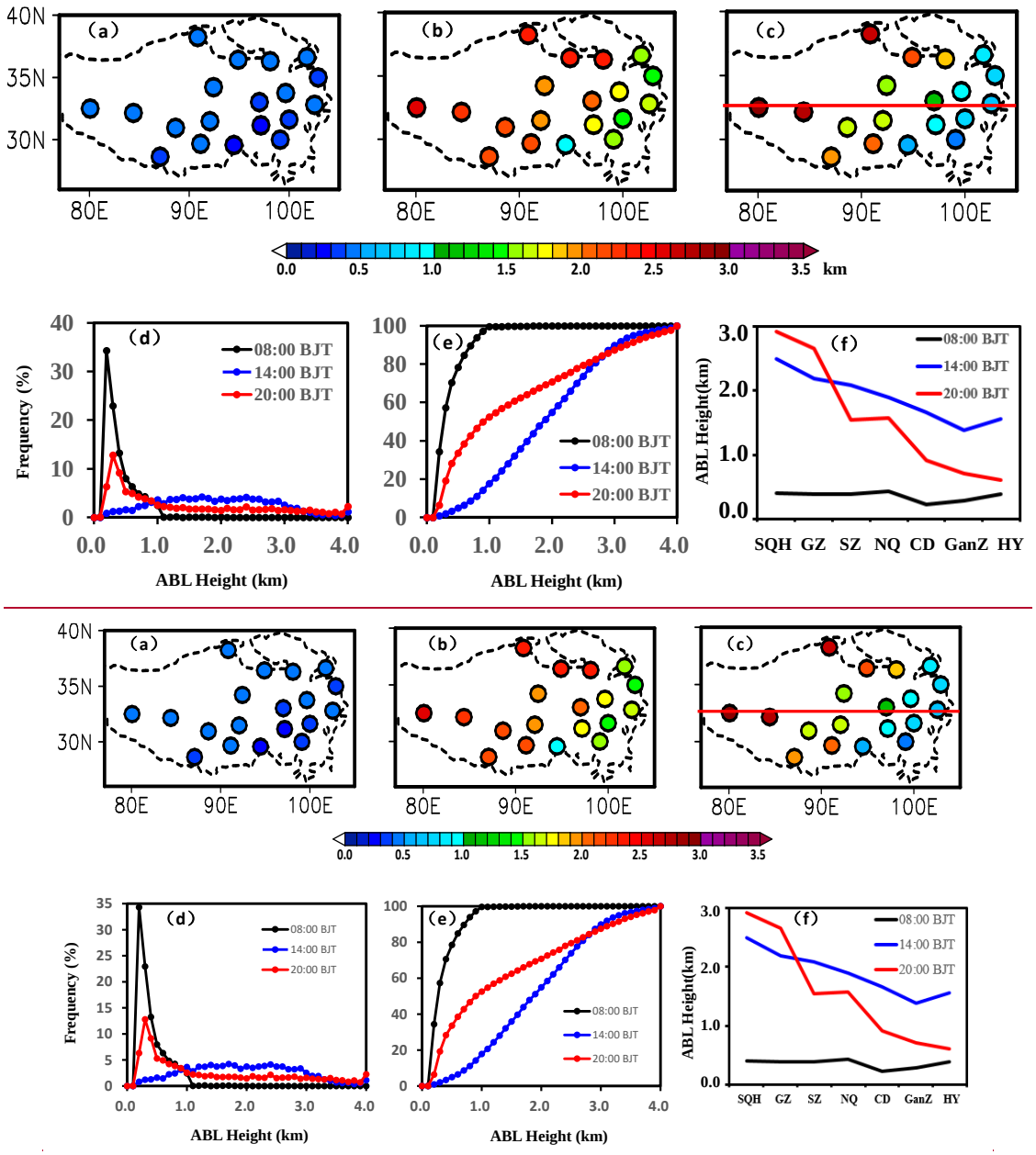

Figure ~~23~~: Spatial distribution of the mean ABL height (ABLH) ~~for all types~~ at (a) 00:08 BJT, (b) 14:00 BJT, and (c) 20:00 BJT ~~in the study period~~; (d) the regional mean frequency and (e) cumulative frequency distributions of the ABLH ~~height over~~ in the TP at 08:00 BJT, 14:00 BJT, and 20:00 BJT; (f) the west-east cross sections of the ABLH ~~height~~ along 32 ℃N (indicated by red line ~~shown~~ in (c)) at 08:00 BJT, 14:00 BJT, and 20:00 BJT.

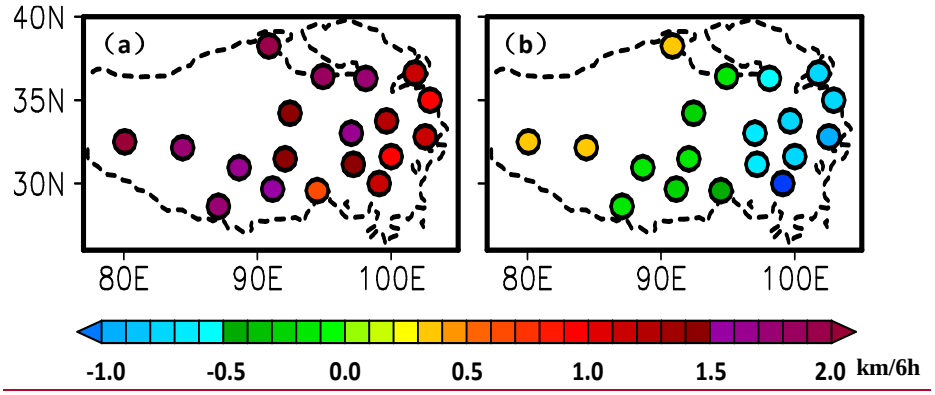

Figure 4: Spatial distribution of the ABLH growth rate from 08:00 BJT to 14:00 BJT (a) and from 14:00 BJT to 20:00 BJT (b).

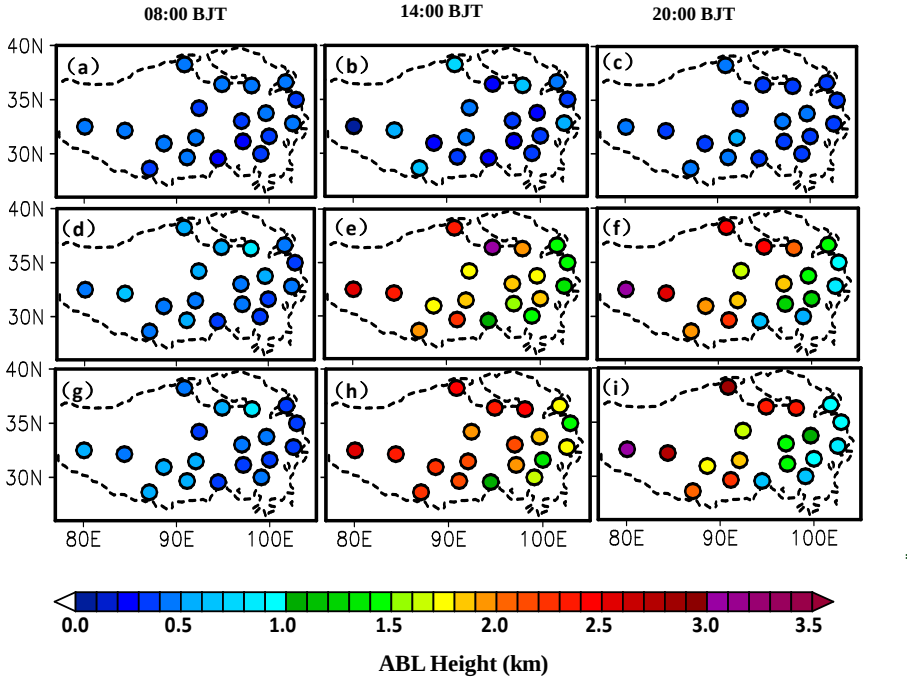

~~Figure 3: Same as in Fig. 2a but for the SBL (top), NBL (middle), and CBL (bottom) at 08:00 BJT, 14:00 BJT, and 20:00 BJT.~~

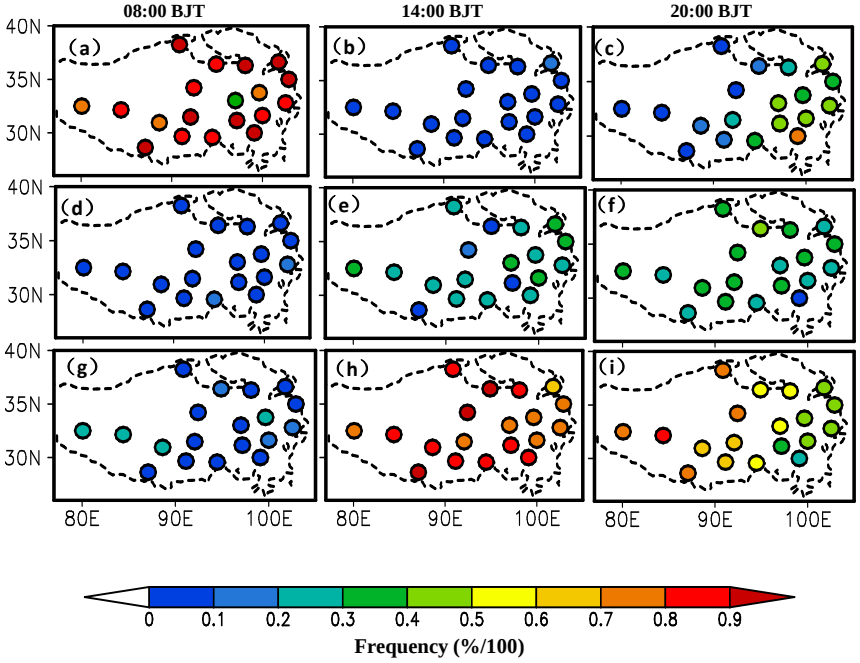

Figure ~~4~~5: Spatial distribution of the occurrence frequency for the SBL (top), NBL (middle), and CBL (bottom) at 08:00 BJT, 14:00 BJT, and 20:00 BJT~~Same as in Fig. 3 but for the occurrence frequency~~.

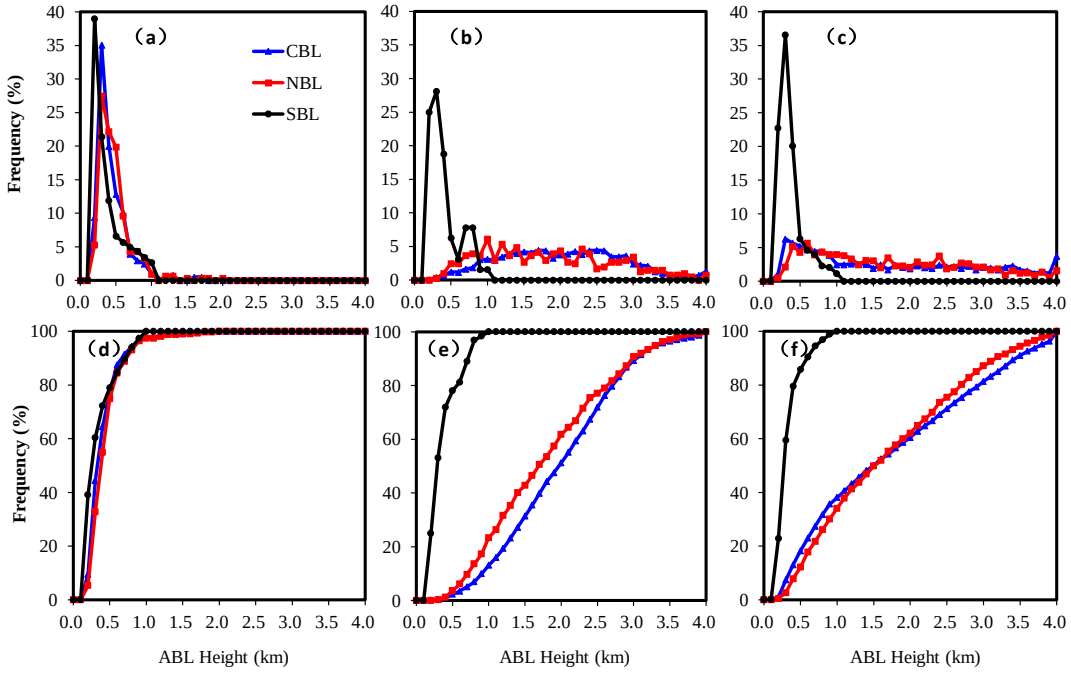

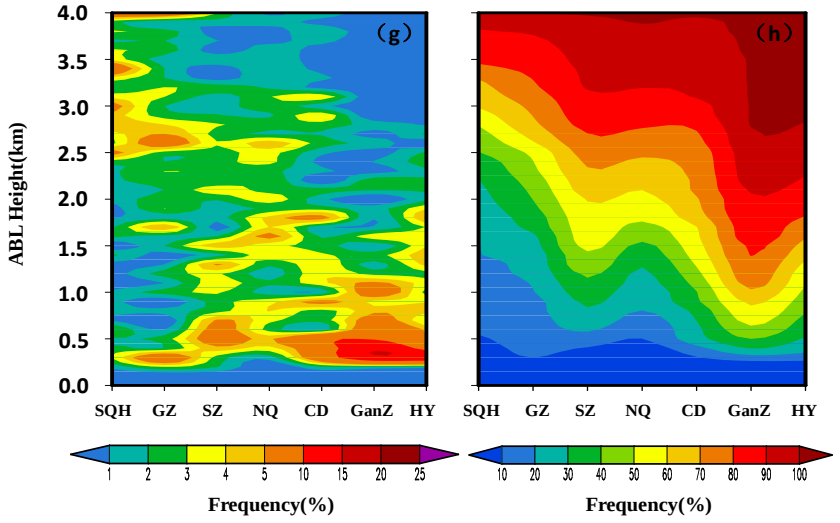

Figure ~~5~~6: The regional mean frequency distributions of the ~~ABL height~~ABLH over the TP for the CBL (blue), NBL (red), and SBL (black) ~~in the study period~~ at (a) 08:00 BJT, (b) 14:00 BJT, and (c) 20:00 BJT; and (d)-(f) same as in (a)-(c) but for the cumulative frequency distributions; and ~~.~~

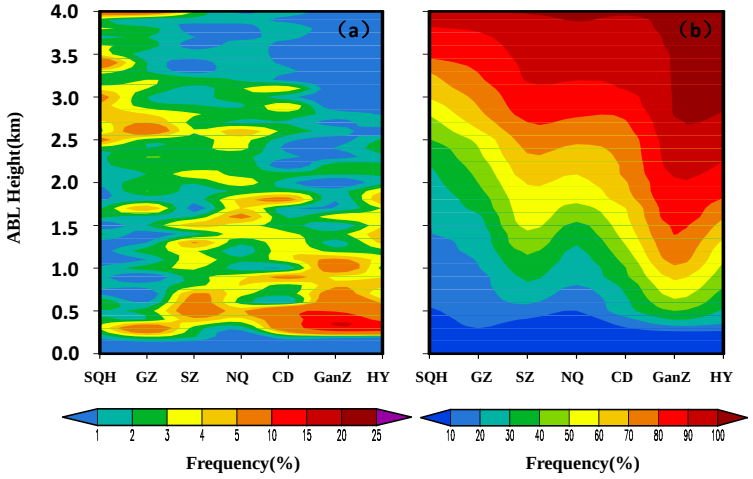

~~Figure 6: T~~the west-east cross sections of frequency (~~a~~g) and cumulative frequency (~~b~~f) distributions of the CBL height along 32 ℃N in daytime (14:00 and 20:00 BJT).

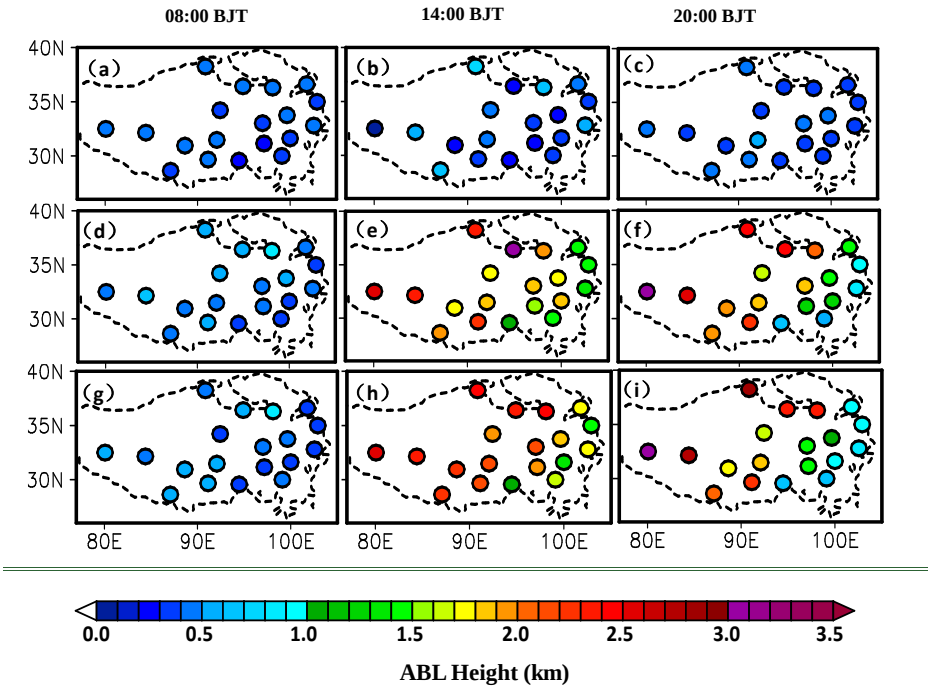

Figure ~~37~~: Spatial distributions of the mean ABLH ~~Same as in Fig. 2a but~~ for the SBL (top), NBL (middle), and CBL (bottom) at 08:00 BJT, 14:00 BJT, and 20:00 BJT.

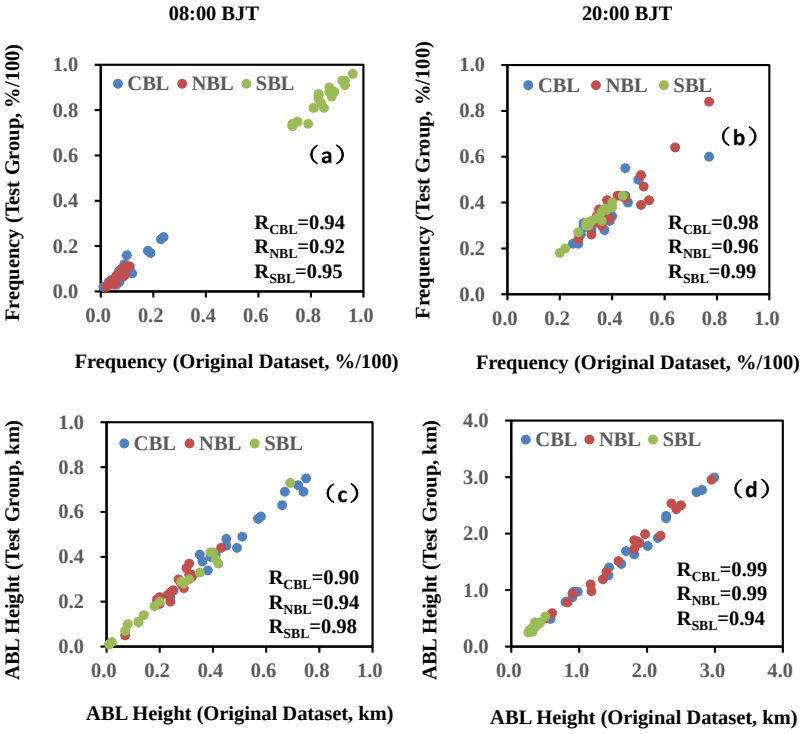

Figure ~~7~~8: The scatter plots of the occurrence frequency of the SBL, NBL, and CBL from the original and test group datasets at ~~each of~~ 19 stations at (a) 08:00 BJT and (b) 20:00 BJT; and (c)-(d) same as in (a)-(b) but for the ABL~~H height~~.

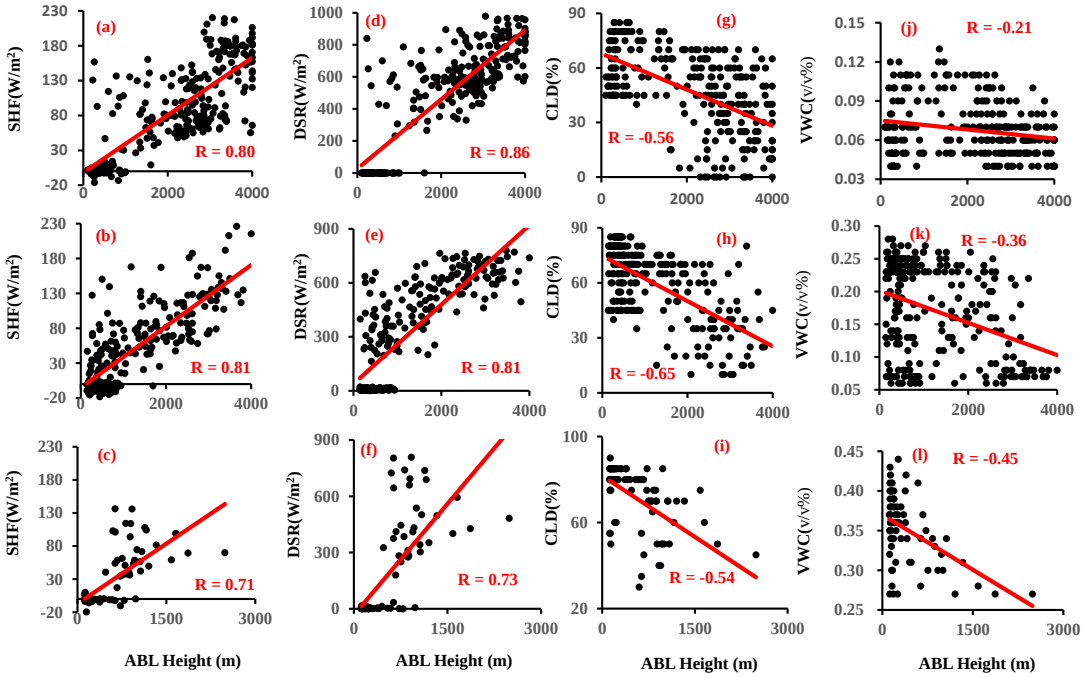

Figure ~~89~~: Scatter plots of the ABLH ~~height~~ and the 6-hour average of surface sensible heat flux (SHF) (a-c), surface downward solar irradiance~~radiation flux~~ (DSR) (d-f), total cloud coverage (CLD) (g-i), and surface soil volume moisture content (VWC) (j-l) at 08:00 BJT, 14:00 BJT, and 20:00BJT at SQH (top), NQ (middle), and LZ (bottom) stations in the study period. The correlation coefficient (R) is given in each panel.

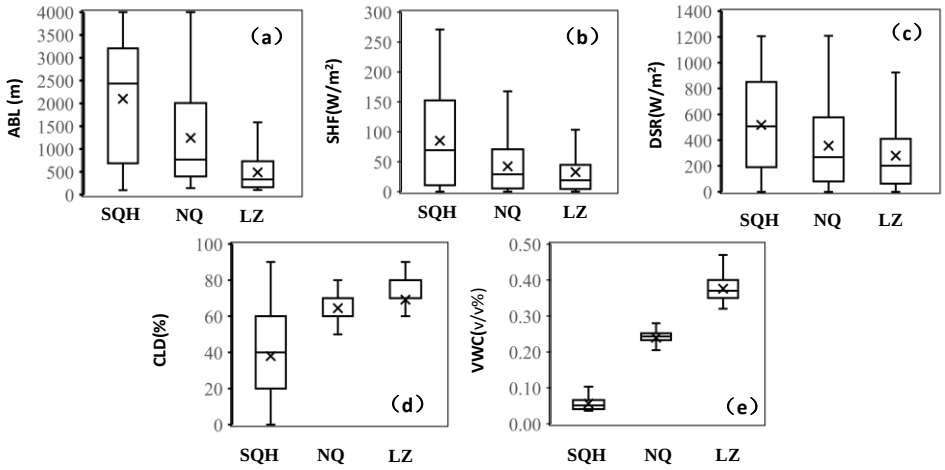

Figure ~~910~~: (a) The ABLH ~~height~~, (b) SHF, (c) DSR, (d) CLD, and (e) VWC at SQH, NQ, and LZ stations in the study period. Horizontal bars show the 5th, 25th, 50th, 75th, and 95th percentile values and "×" symbols show the corresponding mean value.

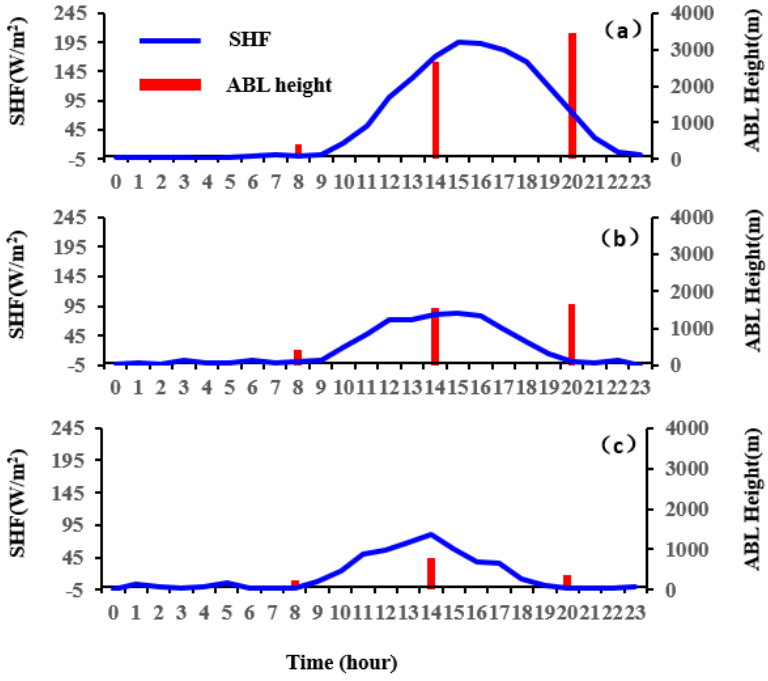

Figure ~~10~~11: Diurnal variations of surface sensible heat flux (blue) and the ~~ABL height~~ABLH (red) averaged over the study period at (a) SQH, (b) NQ, and (c) LZ stations ~~averaged over the study period~~.

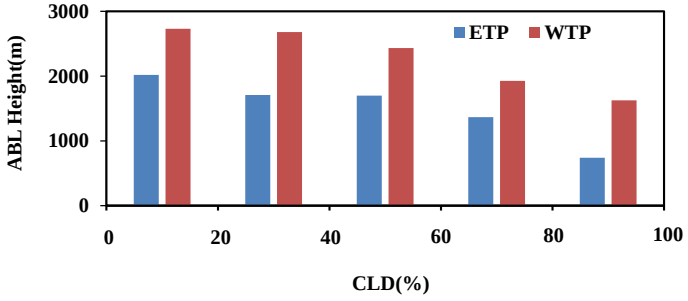

Figure ~~11~~12: The mean ~~ABL height~~ABLH (for the NBL and CBL) and CLD over the ETP (blue) and WTP (red) in daytime (14:00 BJT and 20:00 BJT).

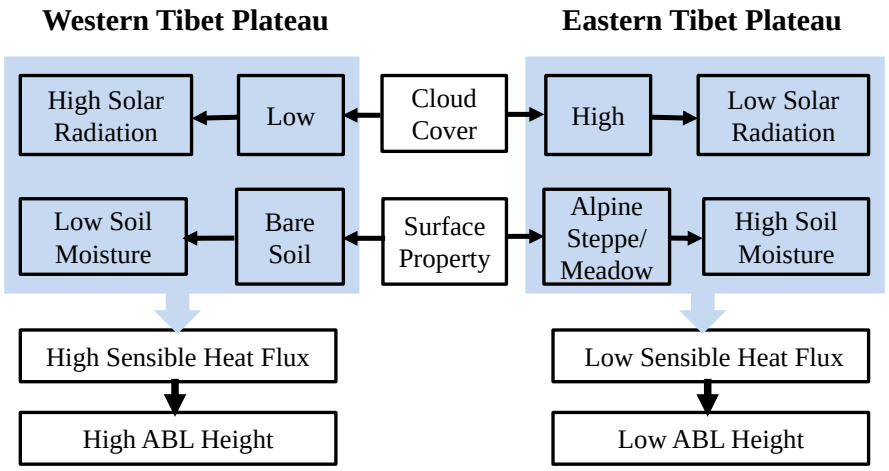

Figure ~~12~~13: A schematic diagram for relationships between the ~~ABL height~~ABLH and the influential factors in the ETP and the WTP.